ornl

ORNL/TM-13334

OAK RIDGE NATIONAL LABORATORY

LOCKHEED MARTIN

MCNP-DSP Users Manual

Timothy E. Valentine

MANAGED AND OPERATED BY
LOCKHEED MARTIN ENERGY RESEARCH CORPORATION
FOR THE UNITED STATES
DEPARTMENT OF ENERGY

ORNL-27 (3-96)

ORNL/TM-13334

Instrumentation and Controls Division

MCNP-DSP Users Manual

Timothy E. Valentine

Date Published— January 1997

Prepared by the
OAK RIDGE NATIONAL LABORATORY
Oak Ridge, Tennessee 37831-6285
Managed by
LOCKHEED MARTIN ENERGY RESEARCH CORP.
for the
U.S. DEPARTMENT OF ENERGY
under contract DE-AC05-96OR22464

CONTENTS

LIST OF FIGURES

LIST OF TABLES

ABSTRACT

The Monte Carlo code MCNP-DSP was developed from the Los Alamos MCNP4a code to calculate the time and frequency response statistics obtained from the ^{252}Cf-source-driven frequency analysis measurements. This code can be used to validate calculational methods and cross section data sets from subcritical experiments. This code provides a more general model for interpretation and planning of experiments for nuclear criticality safety, nuclear safeguards, and nuclear weapons identification and replaces the use of point kinetics models for interpreting the measurements. The use of MCNP-DSP extends the usefulness of this measurement method to systems with much lower neutron multiplication factors.

1. INTRODUCTION

The Monte Carlo code MCNP-DSP[1] was developed from the MCNP4a[2,TM] code to calculate the time and frequency measured parameters of the ^{252}Cf-source-driven noise analysis method.[3] This measurement technique was developed to determine the subcriticality of fissile assemblies. This method also provides measured parameters that can be used for nuclear weapons identification,[4] nuclear materials control and accountability,[5] quality assurance,[6] process monitoring,[7] and verification of calculational methods and cross sections.[8] In the past, point reactor kinetics expressions were used to relate the measured spectra to the subcritical neutron multiplication for criticality safety applications. However, this limited the applications of this measurement technique to systems where point reactor kinetics was applicable.

The KENO-NR[9] Monte Carlo code was developed by Ficaro from KENO V.a[10] to calculate the spectral densities of this measurement. However, this code is limited in that it only calculates the detector responses due to neutrons and uses group cross section, whereas the most efficient detectors used in the measurements detect both neutrons and gamma rays. Sometimes gamma ray detectors are used exclusively in the measurements. Because of these limitations, a more generalized Monte Carlo model which has continuous energy cross sections and which also includes gamma rays was needed to calculate the spectral densities.

To provide a more detailed model for interpretation of the measured results, the Monte Carlo code MCNP4a was modified to calculate both the time and frequency domain signatures from this measurement. Several modifications were made to the neutron and gamma ray tracking routines of MCNP such that the calculated parameters are obtained as measured. The structure of the code was modified to obtain data blocks of detector responses, as in measurements. The data blocks are time samples of detector response, typically of 512 or 1024 points, for a certain period, which is determined from the sampling rate of the data acquisition system. The particle splitting and biasing in MCNP were disabled in order to have a strictly analog Monte Carlo calculation that follows physically the actual particle random walks. A dual-particle source was developed which produces both neutrons and gamma rays from the fission of ^{252}Cf in which the time tracking of the gamma rays was coupled to that of the neutrons. Additional evaluated measured data were incorporated into the code for certain neutron and gamma ray interactions to more precisely follow the physics of particle interaction on an event-by-event basis. Average quantities like $\bar{\nu}$, the average number of prompt neutrons per fission, were removed from MCNP-DSP because average quantities remove some of the statistical fluctuations from the fission chain populations. Experimental data describing the probability distribution of the number of prompt neutrons from fission were incorporated into the code where available; otherwise, the Gaussian theoretical distribution is used. A modified Maxwellian energy distribution was included in the code to obtain the energy of

---

[TM] *MCNP is a trademark of the Regents of the University of California, Los Alamos National Laboratory.*

prompt neutrons from the spontaneous fission of ^{252}Cf along with angular distribution data for neutrons from fission to describe anisotropy of the neutron directions in the laboratory system. The energy distribution of gamma rays from the spontaneous fission of ^{252}Cf and the multiplicity of these gamma rays were also incorporated into MCNP-DSP. MCNP-DSP correlates both the neutrons and gamma rays in time after the fission throughout the fission chain multiplication process. However, as in MCNP, the gamma ray production is not directly correlated to the type of neutron event. Several detector options were included in MCNP-DSP to allow calculation of the responses of the various neutron and gamma sensitive detectors used in the measurements. The detectors used in MCNP-DSP are capture, scatter, or fission detectors. A new simplified algorithm for treatment of multiple scattering events in the scatter detectors was included in addition to multiple scattering of particles between detectors. Data processing algorithms were also incorporated into the code to process the detector responses for both time and frequency analysis. The frequency spectra can be obtained by directly calculating the Fourier transforms of N point blocks of pulses from the detectors and performing a complex multiplication to obtain the autopower spectral densities (APSDs) and the cross-power spectral densities (CPSDs). The APSDs and CPSDs are also obtained by Fourier transforming the autocorrelation and cross-correlation functions. Randomly pulsed neutron measurements are also simulated by calculating the time distribution of detector counts after ^{252}Cf fission.

This manual provides a description of the modifications made to the MCNP4a code and some general information about signal processing. The modifications to the neutron and photon transport processes are described and a brief explanation of the detection process is presented in Chap. 2. A description of the frequency analysis, correlation analysis, and the pulsed neutron calculations are presented in Chap. 3. A short outline of the program flow is presented in Chap. 4. Chapter 5 contains examples for frequency analysis calculations, correlation analysis calculations, and pulsed neutron calculations. It is assumed that the reader is familiar with standard MCNP input. The neutron emission distributions for spontaneous fission isotopes are given in Appendix A, and the neutron energy spectra parameters for spontaneous fission isotopes are provided in Appendix B.

2. MCNP-DSP MODIFICATIONS

Although MCNP is very versatile, several changes were made to the code to accurately estimate the time- and frequency-analysis statistics. A dual-particle source was developed which produced both time-correlated neutrons and gamma rays. The variance reduction features were disabled in order to have strictly analog particle tracking, and the neutron and gamma ray transport routines were modified to better represent the collision physics on an event-by-event basis.

2.1 NEUTRON MODIFICATIONS

Because the ^{252}Cf-source-driven technique measures the behavior of the individual fission chains in a fissile configuration, it is necessary that the calculation be able to adequately simulate the behavior of the individual fission chains. This requires replacing average parameters such as $\bar{\nu}$ with probability distributions because the spectral densities provide statistical estimates of the fission chain fluctuations and because the average quantities reduce the fission chain fluctuations. The proper treatment of the angular distribution of neutrons from fission was also included in the calculation to adequately describe the particle direction from fission for both spontaneous fission and induced fission. The selection of the energy of the neutrons from the spontaneous fission of ^{252}Cf has been modified to incorporate recent improvements in the representation of the prompt neutron energy spectrum. Implementing these changes along with analog neutron tracking allow for the more physical representation of the individual fission chains.

2.1.1 Number of Prompt Neutrons from Fission

The probability of obtaining prompt neutrons from fission, $P(\nu)$, for various fissioning isotopes was functionally described by Terrell.[11] Terrell suggested that the neutron multiplicities are dependent on the fission fragment properties. If a Gaussian distribution of the fission fragment excitation energies is assumed, the cumulative probability of observing ν prompt neutrons from fission is approximated as

$$\sum_{n=0}^{\nu} P(n) = \frac{1}{\sqrt{2\pi}} \int_{-\infty}^{(\nu-\bar{\nu}-1/2+b)/\sigma} e^{\frac{-1}{2}t} dt \ , \qquad (2.1)$$

where b is a small correction factor ($<10^{-2}$) to ensure that the ν's are positive and σ is the root-mean-square width of the initial total excitation-energy distribution (σ = 1.08).[11] Terrell has shown that this distribution function can be used to describe the emission probability for several different fissioning isotopes. In MCNP, the $\bar{\nu}$ obtained from the cross-section data sets is a function of the energy of the neutron that induces the fission. Thus the emission probability that was incorporated into MCNP-DSP is an energy dependent distribution. The Gaussian distribution is an approximation to describe the

prompt neutron emission probabilities at all energies and is used unless additional measured distribution data tables are included for certain isotopes.

An option has been incorporated into MCNP-DSP to use the measured data summarized by Zucker and Holden.[12] Zucker and Holden tabulated the $P(\nu)$ distributions for ^{235}U, ^{238}U, and ^{239}Pu as a function of the energy of the neutron that induces the fission. These distributions are presented in Figs. 2.1 to 2.3. These tabulated data of Zucker and Holden are used by default. The probability distribution data were fit with least-square polynomials to obtain a functional representation of the energy dependence of neutron emission probabilities. The probability distribution data for the spontaneous fission of ^{252}Cf were taken from Spencer's measurements.[13] The probability distribution data for the inherent spontaneous fission sources was taken from Holden and Zucker.[14] The distribution data for ^{252}Cf and the spontaneous fission isotopes are given in Appendix A.

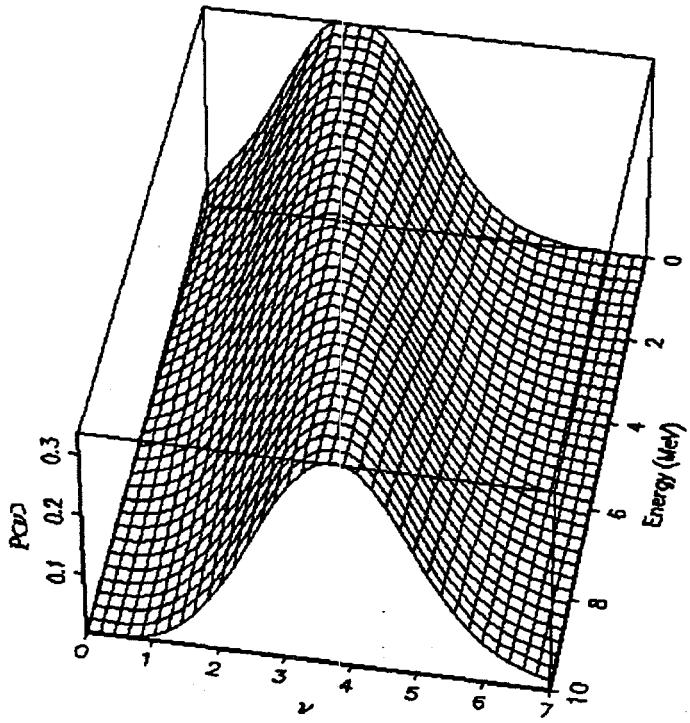

Figure 2.1. P(ν) distribution for ^{235}U

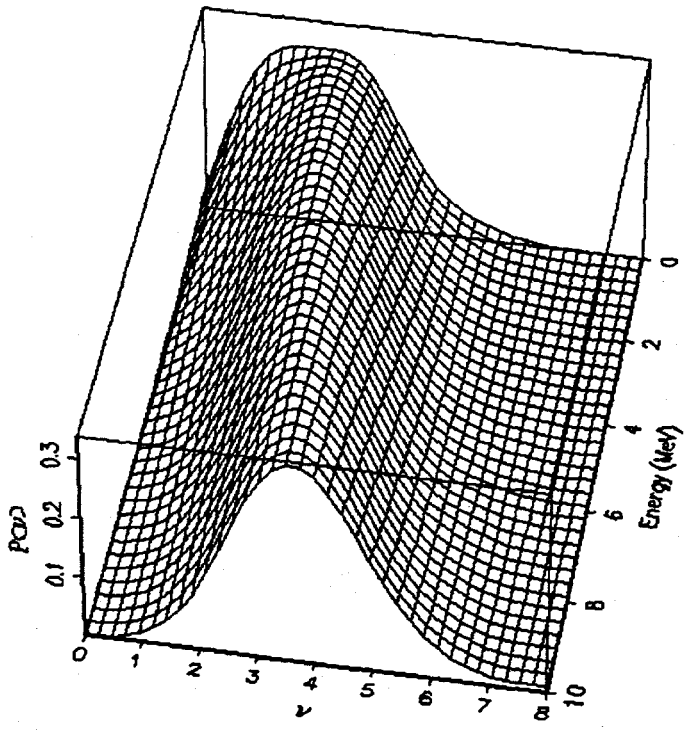

Figure 2.2. P(ν) distribution for ^{238}U

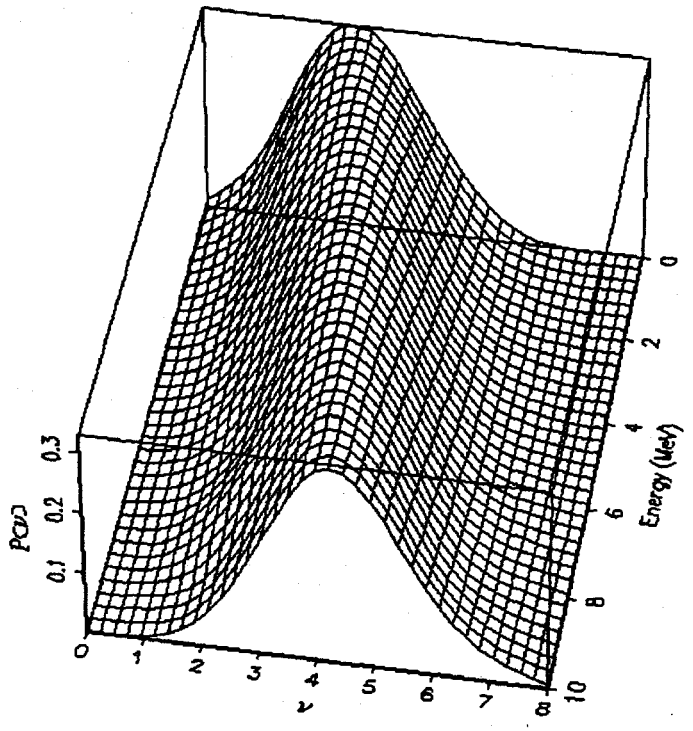

Figure 2.3. P(ν) distribution for ^{239}Pu

2.1.2 Angular Distribution of Prompt Neutrons from Fission

There are instances in which the angular distributions of prompt neutrons from fission may be important, such as when the ^{252}Cf source is located some distance from the fissile configuration. Hence, assuming an isotropic emission of neutrons from fission can be a poor approximation. The angular distribution of neutrons relative to the direction of the light fission fragment has been measured by Budtz-Jorgensen and Knitter[15] for the spontaneous fission of ^{252}Cf. Budtz-Jorgensen and Knitter have shown that there is angular anisotropy in the laboratory reference frame. The probability distribution function obtained from the Budtz-Jorgensen and Knitter data is shown in Fig. 2.4. As can be seen from Fig. 2.4, the angular distribution at zero energy is more isotropic; however, as the neutron energy increases, the angular distribution becomes very anisotropic.

These data are incorporated into MCNP-DSP by selecting the direction of the light fission fragment from an isotropic distribution. The neutron direction is then determined by sampling its azimuthal direction uniformly on the interval 0 to 2π. The polar angle of each fission neutron relative to the light fission fragment is determined from the angular probability distribution function. These data may be used for both the spontaneous fission of the ^{252}Cf source and for induced fissions in the system to investigate the effects of the angular dependence of the neutron emission. Since the majority of the neutrons are released from the fully accelerated fission fragments, the angular distribution of the neutrons relative to the direction of the fission fragments is dependent on the de-excitation of the fission fragments. Therefore, there would be little difference between the angular distribution of spontaneous fission neutrons and the angular distribution of induced fission neutrons for fissile isotopes. For these reasons the data for ^{252}Cf were used for all fission.[16]

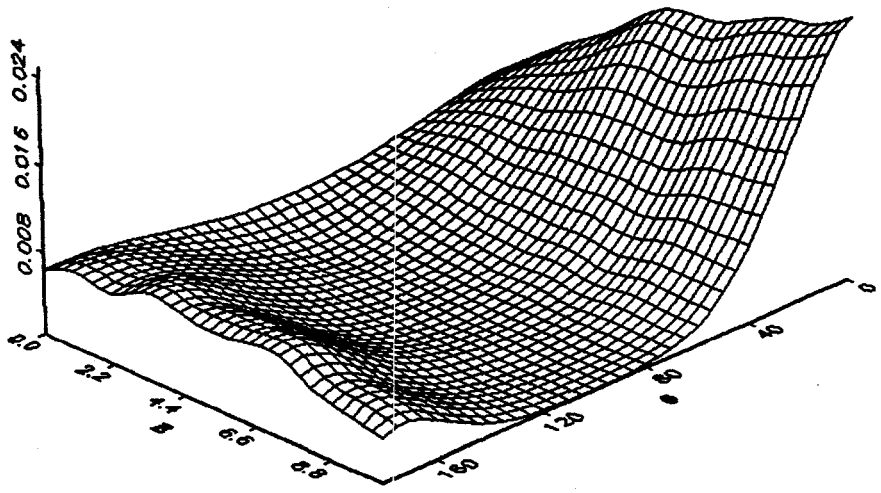

Figure 2.4. Probability density function for angular distribution (lab system) of neutrons from fission with respect to the direction of the light fragment

2.1.3 Fission Neutron Energy Distribution

The neutron energy spectrum is obtained from the nuclear cross-section files for induced fission. A corrected Maxwellian distribution is used for the prompt neutron energy spectrum for ^{252}Cf. A detailed analysis of the experimental data has been performed by Mannhart[17] to obtain the relative difference between the neutron spectrum obtained from the measured data and the Maxwellian distribution for the spontaneous fission of ^{252}Cf. Mannhart developed an energy dependent correction factor for the Maxwellian distribution. The fit to the correction factor data can be found in Appendix B. By multiplying the Maxwellian distribution by the correction factor, an accurate representation of the energy distribution of neutrons from the spontaneous fission of ^{252}Cf is obtained. The average energy obtained from the corrected distribution is 2.13 MeV, which corresponds to the measured value of the average energy of neutrons from the spontaneous fission of ^{252}Cf. An eight-point Gaussian quadrature integration scheme was used to integrate the spectrum from zero to an upper limit of E, where E was varied from 0.00001 eV to 25 MeV. The integrated spectrum was then normalized to unity. The selection of the neutron energy is determined by setting a random number equal to the normalized integrated spectrum and then determining the energy that corresponds to this value of the normalized integrated spectrum. A least-squares polynomial fit of the neutron energy as a function of the value of the normalized integrated spectrum was used. This resulted in an expression for the neutron energy as a function of the normalized integrated spectrum, that is, the neutron energy as a function of the random number. A Watt fission spectrum is used for the spontaneous fission of the inherent fission sources. The parameters for the Watt spectrum can be found in Appendix B.

2.2 MODIFIED GAMMA RAY TRANSPORT

In MCNP, gamma ray production from neutron events is determined by sampling a total gamma ray production cross section. These cross sections contain data on the multiplicity and energy of gamma rays from neutron reactions that produce gamma rays. These reactions include neutron capture, inelastic neutron scattering, and fission. Although the cross sections are measured separately, these gamma-ray-producing reactions are lumped together in the MCNP nuclear data sets. Consequently, these data cannot be easily separated without extensive modifications to the code and the formatted data files. This grouping does not allow the physics of the gamma ray production process to be exact on an event-by-event basis but does give a correct average behavior.[18] This will lead to no uncertainty in the first moment of the populations but may introduce some uncertainty into the second moment on which noise-measured parameters depend, especially when inelastic neutron scattering and fission are equally probable. This may also reduce some of the fluctuating phenomena associated with gamma ray production. The multiplicity and energy distribution of prompt gamma rays from the spontaneous fission of the ^{252}Cf source has been included in MCNP-DSP.

2.2.1 Prompt Gamma Ray Multiplicity for ^{252}Cf

The gamma ray multiplicity, like the neutron multiplicity, is a function of the fission fragment mass but has little dependence on the energy of the neutron inducing the fission. A sawtooth dependence of the gamma ray yield on fragment mass has been observed for the spontaneous fission of ^{252}Cf and for thermal neutron fission of ^{235}U.[19] Since the number of gamma rays emitted is mainly dependent on the fission fragment properties, a single distribution can be used to describe the gamma ray multiplicity for ^{252}Cf.

The gamma ray multiplicity was determined using Brunson's[20] measurements, which fitted the data to a double Poisson model. Brunson's model depends on the minimum energy of the gamma rays emitted. For a minimum energy of 85 keV, the resulting probability distribution is used to obtain the gamma ray multiplicity

$$\Pi(G) = 0.682\frac{7.20^G e^{-7.20}}{G!} + 0.381\frac{10.71^G e^{-10.72}}{G!} \quad . \qquad (2.2)$$

where G is the gamma ray multiplicity. The gamma ray multiplicity ranges from 0 to 20 gamma rays per fission with an average value of 7.79 gamma rays per fission. This value does not differ greatly from that obtained by others.[20]

2.2.2 Prompt Gamma Ray Energy Distribution for ^{252}Cf

The gamma ray energy spectrum has been measured for the spontaneous fission of ^{252}Cf and the thermal-neutron-induced fission of ^{235}U. There appears to be little difference between the spectrum from ^{252}Cf and that from ^{235}U.[21] Because of the small difference between the two spectra and because the measurements of the ^{235}U gamma ray spectra are more precise, the gamma ray spectra from the thermal neutron fissioning of ^{235}U is used to obtain the gamma ray energy.

The energy spectrum of the prompt fission gamma rays is obtained from Maienschein's measurements.[22,23] From 0.3 to 1. MeV, the distribution is described as

$$N(E) = 26.8e^{-2.30E} \quad . \qquad (2.3)$$

In the interval 1.0 to 8.0 MeV, the distribution is described as

$$N(E) = 8.0e^{-1.10E} \quad . \qquad (2.4)$$

The upper energy limit of 8 MeV was selected because nuclear excitation above 8 MeV typically leads to neutron rather than gamma emission. Although Maienschein's

experiment determined the gamma ray spectrum down to 0.25 MeV, there are several gamma ray energies that show preferential emission for low multiplicities below 0.3 MeV.[20] On the advice of Ray Nix,[16] the spectrum below 0.3 MeV is represented as

$$N(E) = 38.13(E - 0.085)e^{1.648E} . \quad (2.5)$$

The minimum gamma ray energy of 0.085 MeV coincides with Brunson's measurements. Below this energy, gamma ray emission is due to K-shell X rays from the fission fragments that occur later than the prompt gamma emission from fission. Using this functional representation of the prompt fission gamma ray energy spectrum, a value of 0.898 MeV is obtained for the average gamma ray energy per fission. This value agrees well with the accepted value of 0.88 MeV per fission.[20]

Some correlation exists between the total gamma ray energy release and the number of neutrons emitted from fission. Nifenecker[24] has observed that there is competition in the de-excitation mechanism of the fission fragments. This can be expected since it has been shown that the angular momentum of the fission fragments is transferred to the gamma rays and essentially no angular momentum is given to the neutrons as a consequence of selection rules.[19] Nifenecker obtained the following linear relationship between the number of neutrons emitted from fission, ν, and the total gamma ray energy, E_t:

$$E_t = 0.75\nu + 4 . \quad (2.6)$$

This relationship can be used to put a limit on the total gamma ray energy from the spontaneous fission of the ^{252}Cf source and also couples the gamma ray production with the neutron production.

2.3 PARTICLE DETECTION

Although MCNP is capable of tracking electrons, the electron production and subsequent light production in the detectors were not treated rigorously. An intuitive approach was used to determine when particles contribute to the detector response. This approximation faithfully reproduces the measured detector responses. Currently, three detector types can be employed in a calculation: capture, scatter, or fission detectors.

2.3.1 Neutron Detection

In the MCNP-DSP calculation, neutron detection is characterized by a particular neutron event. The detector response of capture detectors is primarily due to the absorption of a neutron with the subsequent emission of secondary charged particles, which ionize the detection media and produce an electronic pulse proportional to the kinetic energy of the secondary charged particle. These detectors typically have a very large thermal neutron absorption cross section and a very small scattering cross section.

In MCNP-DSP, if a neutron is absorbed in a capture detector, a count is scored in the appropriate time bin, and the number of detections is incremented.

Scattering detectors are those in which the response is due primarily to neutron scattering in the detection media. To observe a count in a scattering detector, the neutron must transfer a certain preselected amount of energy to the detection material via the kinetic energy of the recoil nucleus, which excites electrons in the scintillation material which produce light that is converted into an electrical pulse by a photomultiplier tube. Although MCNP can handle this scintillation process directly, an intuitive approximation was utilized which assumes that the light production is proportional to the energy deposited by the neutron. An energy threshold is specified in the calculation for each detector. Since multiple neutron scattering can occur in the detector, special attention was given to modeling the multiple scattering in these detectors by specifying a time width, the pulse generation time, in which energy contributions from the events are summed together. If a neutron scatters in the detector and deposits an amount of energy greater than the neutron threshold, a count is registered, and additional neutron scatters within the specified pulse generation time of the detector are ignored. However, if the amount of energy deposited in the detector is less than the neutron threshold, the energy of the subsequent neutron scatters in the detector are added together for those events that occur within the pulse generation time of the detector. To account for neutrons that may scatter between adjacent detectors several times, the time at which the neutron had its last scattering event in each detector is stored for each neutron track.

In fission detectors, the fission fragments travel through the detection media, ionizing the atoms in the detector. The large energy release per fission allows for easy discrimination of other events that may also produce ionized atoms in the detector. In the calculation, a count is registered each time a fission occurs in the detection media, and the fission neutrons are stored for tracking. The fission detectors may be used for other applications of interest such as time- and frequency-analysis studies.

2.3.2 Gamma Ray Detection

Various gamma ray events may lead to a detection in the capture and scattering detectors since the gamma ray events also produce secondary charged particles. If the gamma ray energy deposited is above a certain threshold, which is specified as input to the calculation, gamma ray absorption due to the photoelectric effect can lead to a detection. Likewise, if the gamma ray has an incoherent scatter in the detector and the recoil electron has an energy greater than the threshold, a detection will occur. Multiple scattering of gamma rays in the detector media is treated much in the same way as for neutrons.

3. CALCULATIONAL MODES

There are three calculation modes that are available with MCNP-DSP. These are frequency analysis, correlation analysis, and pulsed neutron calculations. All of these modes of analyses are related and constitute part of the ^{252}Cf-source-driven noise analysis method. This chapter begins with a general description of the ^{252}Cf-source-driven noise analysis measurement as an introduction to the method followed by a description of frequency analyses, correlation analyses, and pulsed neutron calculations.

3.1 ^{252}CF-SOURCE-DRIVEN NOISE ANALYSIS METHOD

This measurement method two or more particle detectors along with a ^{252}Cf source to provide measured quantities that can be used to characterize subcritical fissile assemblies. The source, which is contained within an ionization chamber and designated as detector 1, is placed in or near the subcritical fissile configuration to initiate the fission chain multiplication process. For each spontaneous fission of ^{252}Cf, an electrical pulse is produced that indicates the time of fission and emission of neutrons and gamma rays. The particle detectors, designated as 2, 3, etc., are placed in or near the fissile assembly to measure particles from the fission chains induced by the spontaneous fission of the ^{252}Cf source. The signatures obtained from this measurement are the APSDs of the source and detector signals, the CPSDs between the source and detectors, and the CPSD between detectors. The APSD of the source, $G_{11}(\omega)$, is proportional to the disintegration rate of the source, and the APSDs of the detectors, $G_{22}(\omega)$ and $G_{33}(\omega)$, are proportional to the count rate of the detectors. The CPSDs between the source and the detectors, $G_{12}(\omega)$ and $G_{13}(\omega)$, are proportional to the induced fission rate in the system, and the CPSD between detectors, $G_{23}(\omega)$, is proportional to the induced and inherent fission rate in the system. The APSDs and CPSDs are defined by performing a complex multiplication of the Fourier transform of the blocks of detector signals. The APSD is defined as

$$G_{xx}(\omega) = X^*(\omega)X(\omega) \ , \tag{3.1}$$

where $X(\omega)$ is the Fourier transform of the detector signal and * denotes the complex conjugate. Similarly, the CPSD between two signals x(t) and y(t) is defined as

$$G_{xy}(\omega) = X^*(\omega)Y(\omega) \ . \tag{3.2}$$

The APSDs and CPSDs can also be obtained by Fourier transforming auto- and cross-correlation functions. The autocorrelation function is defined as

$$\phi_{xx}(\tau) = \lim_{T\to\infty} \frac{1}{2T} \int_{-T}^{T} x(t)x(t+\tau)dt \ , \tag{3.3}$$

where $x(t)$ is the detector time response. The APSD is then defined as

$$G_{xx}(\omega) = \int_{-\infty}^{\infty} \phi_{xx}(\tau) e^{-j\omega\tau} d\tau \ . \tag{3.4}$$

Similarly, the cross-correlation between two signals is defined as

$$\phi_{xy}(\tau) = \lim_{T\to\infty} \frac{1}{2T} \int_{-T}^{T} x(t) y(t+\tau) dt \ . \tag{3.5}$$

The CPSD is then defined as

$$G_{xy}(\omega) = \int_{-\infty}^{\infty} \phi_{xxy}(\tau) e^{-j\omega\tau} d\tau \ . \tag{3.6}$$

A certain ratio of spectral densities, $R(\omega)$, is independent of detector efficiency and source intensity (as long as there are no intrinsic or other significant sources of detected events other than from particles from fissions induced in the fissile configuration by the ^{252}Cf source). The ratio of spectral densities is defined as

$$R(\omega) = \frac{G_{12}^{*}(\omega) G_{13}(\omega)}{G_{11}(\omega) G_{23}(\omega)} \ , \tag{3.7}$$

where ω is the angular frequency and the * denotes complex conjugation. Another useful quantity is the coherence,

$$\gamma_{ij}^{2} = \frac{\left|G_{ij}(\omega)\right|^{2}}{G_{ii}(\omega) G_{ij}(\omega)} \ , \tag{3.8}$$

which is the fraction of common information between two signals i and j.

As previously discussed, the APSDs and CPSDs may be obtained from the measurement by direct Fourier processing of the detector signals or by calculating correlation functions and then calculating the frequency spectra. For direct frequency analysis, the detector signals after amplification are input to discriminators, which are used to eliminate unwanted detector pulses. The signal pulses from the discriminator are input into a circuit that converts them into voltage pulses that have a constant area and a frequency spectrum defined by an adjustable RC time constant. The signals are then passed through a low-pass filter, which eliminates the upper frequency components that are greater than half the sampling rate. This prevents aliasing from occurring during the discrete Fourier processing of the signals. Aliasing is the folding of high frequencies over to the low frequency when the sampling rate is less than twice the maximum frequency of

the signal.[25] The filtered signal is digitized repeatedly by an analog-to-digital converter to provide an integer value proportional to the voltage of the signal. The digitized data are divided into segments, termed data blocks, of typically 512 or 1024 points, and then the data are Fourier transformed. The APSDs and CPSDs are calculated for each data block by complex multiplication of the transformed data. The latest estimates are then averaged with the previous data to obtain the current APSDs and CPSDs. This process is continued until the desired convergence is reached.

In correlation measurements, the detector signals from the discriminators are sent into a processor that collects the signals in 512 time bins, a data block. The correlation functions are calculated for each data block and averaged with previous estimates of the correlation functions. After all data blocks have been calculated, the average correlation functions are Fourier transformed to obtain the average APSDs and CPSDs. After obtaining the average APSDs and CPSDs, the coherences and the ratio of spectral densities are calculated as before.

The pulsed neutron measurement is related to the correlation domain measurement. In the correlation and frequency domain measurements, the spontaneous fission of the source occurs randomly in the data block; however, in pulsed neutron measurements operating in the forward mode, a time-to-amplitude converter (TAC) is triggered with the source event and stopped with the detector anode signal from the discriminator. The TAC output is sent into a multichannel analyzer to obtain the neutron and gamma ray time-of-flight. The time-of-flight is the impulse response function for the system and is equivalent to the cross correlation between the source and the detector.

3.2 FOURIER ANALYSIS

The frequency analysis calculation incorporates some of the filtering and windowing options used in the measurements. In the measurements, prior to sampling into the data block, the detector signals are input to a bandpass filter to prevent aliasing. To simulate the bandpass filter, two filter options can be employed in the calculation. Rockland and Precision filters were used in the measurements; hence, functions that represent these filters may be used in the calculations. The Rockland filter function is shown in Fig. 3.1, and the Precision filter function is presented in Fig. 3.2. The peak values of the filter functions are normalized to one. The upper frequency cutoff is set equal to 40% of the sampling rate as implemented in the measurement to prevent aliasing. These filter functions are applicable only for sampling rates less than 100 kHz since the low-pass filter has not been included in the model and its time response affects the detector response for sampling rates greater than 100 kHz. Other higher frequency filter functions could easily be incorporated into the code if the waveforms are available. The time when a particle is detected is determined by adding its time of birth to the time that the particle spent in the system before being detected. A count is registered in the appropriate time bin whose width is determined from

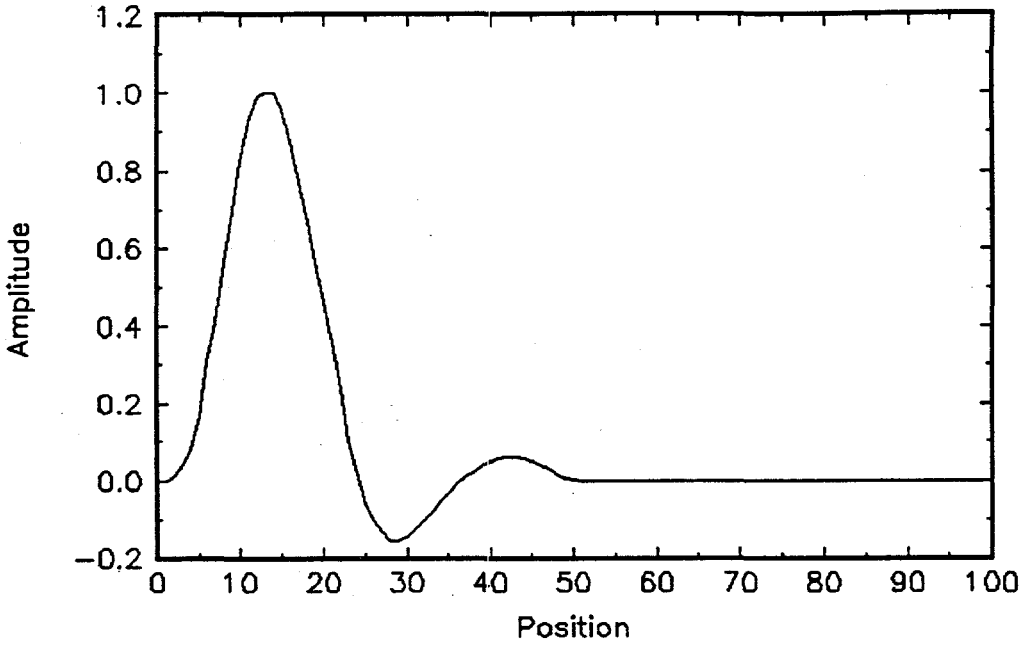

Figure 3.1. Rockland filter function

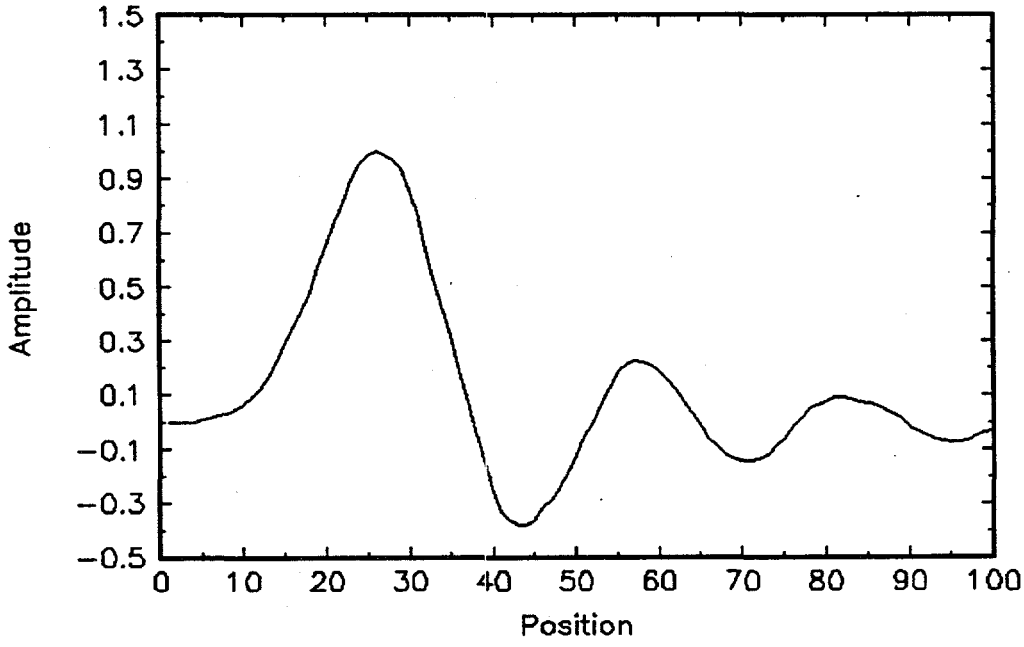

Figure 3.2. Precision filter function

the inverse of the sampling rate. If the filter functions are used, the pulse is spread out over approximately ten time bins for each particle detection. For each time bin, the filter function is segmented into ten discrete values that begin at the time of detection. The digitized values of the normalized filter function that occurs at the right boundary of the time bin are added to the detector time response for that bin. If the particle detection occurs near the end of the data block, the digitized values in the time bins beyond the length of the data block are ignored. Experimentally, the low-frequency components of the detector signal are eliminated by ac coupling (high-pass filtering). To simulate the implementation of a high-pass filter, the average counts per bin are subtracted for each detector's time spectrum for each data block. The removal of the mean value is performed independently of the implementation of the low-pass filter. There are three commonly used windows that may be employed in the calculation. Windows are applied to the time spectra to correct for errors due to the finite length of the data block that coincides with a finite length Fourier transform. The windowed time signal is given by

$$x'(n) = x(n)w(n) \ , \tag{3.9}$$

where $x(n)$ is the discrete detector time signal, and $w(n)$ is the window function. Bartlett, Hanning, and Hamming windows are available in the calculations and are given by[25]

$$w(n) = \begin{cases} 2n/N, & 0 \le n \le N/2 \\ 2 - 2n/N, & N/2 < n \le N \\ 0, & \text{otherwise} \end{cases} \tag{3.10a}$$

$$w(n) = \begin{cases} 0.5 - 0.5\cos(2\pi n/N), & 0 \le n \le N \\ 0, & \text{otherwise} \end{cases} \tag{3.10b}$$

$$w(n) = \begin{cases} 0.54 - 0.46\cos(2\pi n/N), & 0 \le n \le N \\ 0, & \text{otherwise} \end{cases} \tag{3.10c}$$

where N is the length of the data block. A Hanning window has been used in the measurements. A discrete Fourier transform is applied to the data block of length N. The discrete Fourier transform (DFT) is defined as

$$X(k) = \sum_{n=}^{N-} x(n)W_N^{kn} \ , \tag{3.11}$$

where $W_N^{kn} = e^{-j2\pi kn/N}$ is the complex quantity. Because the DFT is a complex function, the estimates of the APSDs and CPSDs are obtained by complex multiplying the DFT of the detector responses for each data block. The APSDs and CPSDs are calculated for each

data block and averaged with the values from the previous data blocks. The coherences and the ratio of spectral densities may be calculated using the average APSDs and CPSDs.

3.3 CORRELATION ANALYSIS

The calculation of the autocorrelation and cross-correlation functions was included in the code. The code calculates circular correlation functions from the detector time response since this is equivalent to performing the complex multiplication in the frequency domain.[25] The estimate of the circular autocorrelation function is given by

$$R_{xx}(r) = \sum_{k=0}^{N-1} x_k x_{(N-(r-k))}, \tag{3.12}$$

where x is the detector signal, r is the lag index, and N is the number of points per data block. The detector signal is assumed to be periodic $[x_k = x_{(N+k)}]$ the circular correlation function is calculated. Likewise, the estimate of the circular cross-correlation function is given by

$$R_{xy}(r) = \sum_{k=0}^{N-1} x_k y_{(N-(r-k))}, \tag{3.13}$$

where x and y are two different detector signals. Average values of the autocorrelation and cross-correlation functions are calculated as the data blocks are updated. The one-sided APSD is estimated as

$$G_{xx}(m) = 4\left[R_{xx}(0) + \sum_{k=1}^{N-1} R_{xx}(k)\cos(2\pi mk / N)\right], \tag{3.14}$$

for $m = 0,1...,N/2$. Because the cross-correlation function is not symmetric, the CPSD will be a complex quantity. The one-sided CPSD is

$$G_{xy}(m) = C_{xy}(m) - jQ_{xy}(m), \tag{3.15}$$

where

$$C_{xy}(m) = 2\left[\sum_{k=0}^{N-1} R_{xy}(k)\cos(2\pi mk / N) + \sum_{k=0}^{N-1} R_{yx}(k)\cos(2\pi mk / N)\right], \tag{3.16}$$

and

$$Q_{xy}(m) = 2\left[\sum_{k=1}^{N-1} R_{xy}(k)\sin(2\pi mk / N) - \sum_{k=1}^{N-1} R_{yx}(k)\sin(2\pi mk / N)\right], \tag{3.17}$$

for $m = 0,1...,N/2$. These estimates of the APSDs and the CPSDs are then used to calculate the coherence functions and the ratio of spectral densities.

3.4 PULSED NEUTRON

The randomly pulsed neutron measurement with ^{252}Cf is simply a measurement of the impulse response of the system being analyzed. For fissile systems, the ^{252}Cf source induces fissions in the system that can be detected with a neutron detector. The resulting time-dependent detector signature consists of a transmission component, a scattered component, and a fission component. This measurement is simulated by starting the source particles at time zero and tracking the source particles and their progeny to the detector. The time of detection for each particle is determined and the counter for the appropriated time bin is incremented much like the accumulation of the pulse height spectra with a multichannel analyzer. For a single "hit" measurement system, only one detector count triggers the TAC for each ^{252}Cf fission; however, in the calculations, all detector counts for a given ^{252}Cf fission are stored.

4. MCNP-DSP PROGRAM FLOW

The general structure of MCNP has been preserved as much as possible. However, some modifications had to be made in order to obtain the frequency data in a manner similar to the measurement. The general flow of MCNP4A is shown in Fig. 4.1. The program starts by reading the command line to determine which options the code uses. After determining the options, the program begins execution. The first step is to read the input file, which can be stated on the command line or the default input file name, *INP*. The arrays are initialized with a call to subroutine *IMCN*. If the frequency analysis calculation is to be performed, a separate data file containing options used in the noise calculation is read in *IMCN*. After initializing the arrays, the interactive geometry plot subroutine *PLOTG* is called if the command line contains *IP* and the options to plot the geometry. Next, the cross-section data are read into the appropriate arrays. Once the cross-section data have been placed in the arrays, the code begins the actual tracking of the particles by calling subroutine *MCRUN*. Subroutine *MCRUN* runs the particle histories by calling *TRNSPT*, which, in turn, calls *HSTORY* to follow the particle tracks throughout the system and writes the detector information. Finally, the tallies are plotted with a call to *MCPLOT* after all the particles have been analyzed. This general structure has been maintained in the modified code. The major difference occurs in the actual transporting of the particles. The subroutine *TRNSPT* has been modified to call *HSTORYCF* if the noise calculation is to be performed.

The structure of the noise calculation is based on an outer and an inner loop. The outer loop controls the number of blocks of data (*bks*) to be calculated. The average number of source events per data block (*scd*) controls the inner loop. If the inherent spontaneous fission source option is invoked, there is a second inner loop that is controlled by the average number of inherent spontaneous fissions per block (*sfpd*). Because spontaneous fission is a Poisson process, the number of disintegrations per block (*ncdis*) is calculated from a Poisson distribution with mean *scd* for the source events per block and with mean *sfpd* for the inherent fission source fissions per block. The ratio of the ^{252}Cf source fission rate to the inherent source fission rate must be known to specify *scd* and *sfpd*. Detected particles from induced fission caused by the inherent source neutrons contribute correlated information to G_{23} but also contribute uncorrelated information to G_{12} and G_{13}. The average number of source events per data block is related to the actual source size by the following relation[12]

$$scd = \frac{mR_{sf}ntbn}{f_s}, \tag{4.1}$$

where m is the mass of the source in micrograms, R_{sf} is the spontaneous fission rate of the source per microgram, *ntbn* is the number of points per block, and f_s is the sampling rate. Using this expression, the source specified in the calculation can be related to the actual source used in the measurements. For calculations employing the inherent fission source option, it has been shown that it is not necessary to use the actual R_{sf} but only maintain

the ratio of *scd* and *sfpb*. The particle tracking begins with the first data block. First, the source particles and their

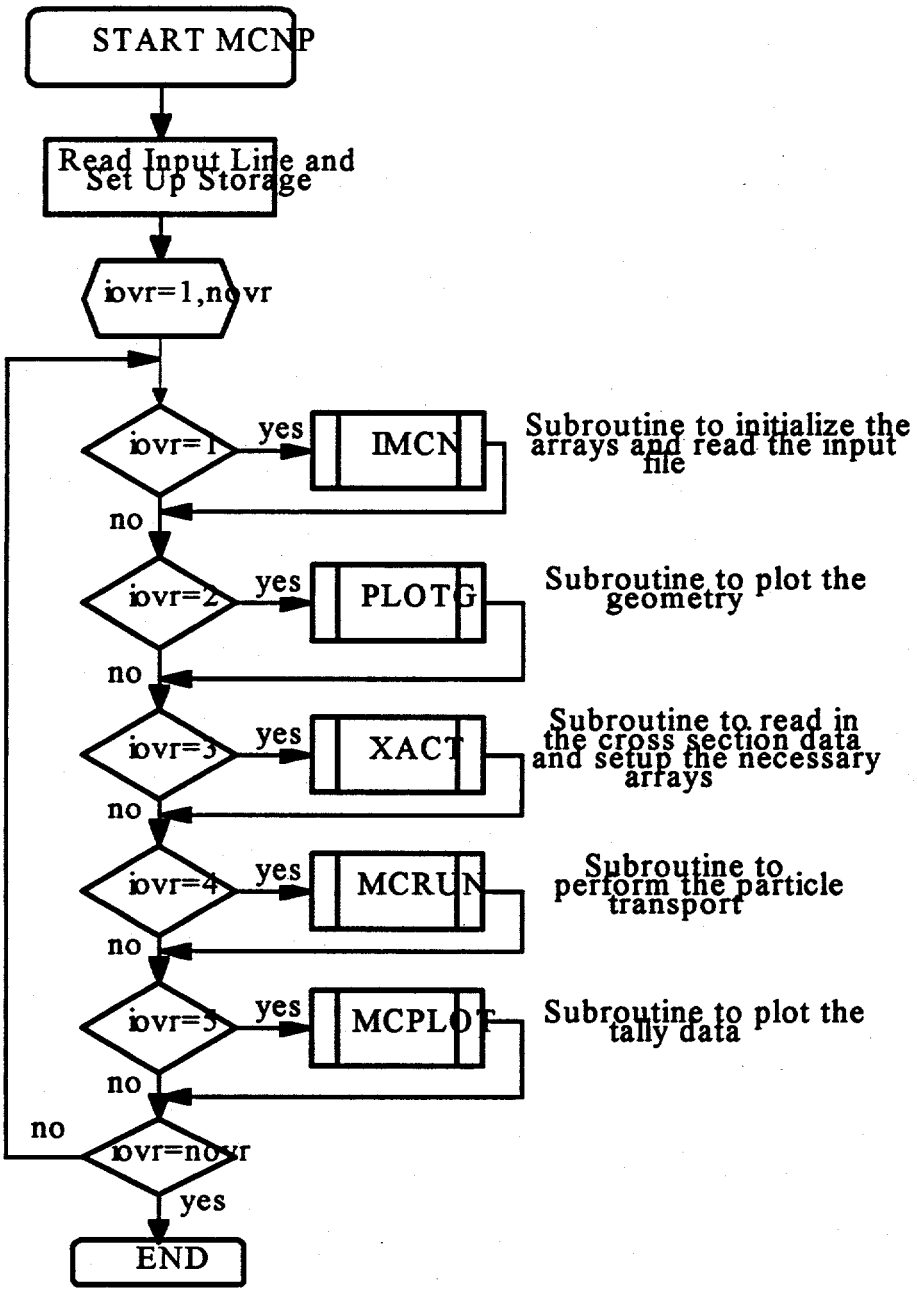

Figure 4.1. General MCNP4a program flow

progeny are tracked. Next, the particles from the inherent fission source and their progeny are tracked if this option is invoked. When the inner loops are finished, the block data are processed. This processing could be the direct calculation of the power spectral densities

or the calculation of the correlation functions. After the block data have been processed, the outer loop variable is incremented and the inner loops are restarted. When all of the data blocks have been calculated, the outer loop is completed. The summary information is written to the output files, and if the data were processed in the correlation function mode, the power spectral densities are calculated and written to a file. This process is depicted in Fig. 4.2.

Since the inner loops control the actual particle transport, a detailed description of the particle tracking follows. The inner loop begins by obtaining information about the source particles. The position is specified in the extra data file for the source particles and is chosen randomly in a specified volume for the inherent fission source. The time of the spontaneous fission is chosen randomly in the data block. The number of particles from the source is chosen randomly. Spencer's distribution is used to obtain the number of prompt neutrons from the ^{252}Cf source, and Brunson's distribution is used to determine the number of prompt gamma rays from the ^{252}Cf source. Zucker and Holden's data are used to determine the number of prompt neutrons from the inherent spontaneous fission source. The energies of the ^{252}Cf neutrons are chosen from the corrected Maxwellian distribution, and the energies of the ^{252}Cf gamma rays are chosen from Maienschein's spectrum. The energy spectra of the inherent fission source neutrons are chosen from the usual MCNP Watt fission spectrum. The direction of the source neutrons can be chosen isotropically or from the angular distribution data of Budtz-Jorgensen and Knitter. All but one of the particles are stored in the bank. An overview of the particle tracking is shown schematically in Fig. 4.3. The distance to the cell boundary, d_b, is determined from the particle's starting location and the direction cosines. Next, the distance to the collision site, d_c, is calculated from the usual relation $d_c = -1n\ R/\Sigma_t$, where R is a random number and Σ_t is the total macroscopic cross section. The minimum distance determines whether or not the particle has a collision. If d_b is less than d_c, the particle is transported through the cell boundary, where the distance to the next cell boundary and the distance to collision are calculated for the new cell. If the particle enters a region of zero importance (outside the system), the particle is said to have leaked, and the leakage tallies are updated. If d_c is less than d_b, then the particle collides in the cell. When a particle collides, the collision nuclide is selected randomly from the materials present in the cell. If the particle is a neutron, the velocity of the collision nuclide is calculated, and the collision event is determined. The capture probability is calculated in the usual way. If the problem is a dual neutron-gamma ray calculation, gamma rays may be produced by the neutron interaction. If the particle is not lost by capture, the neutron will have either an elastic collision or an inelastic collision.[a] The probability of having an elastic collision is given by $\sigma_{el}/(\sigma_{el} + \sigma_{in})$, where σ_{el} is the microscopic elastic scattering cross section and σ_{in} is the microscopic inelastic cross section. The type of inelastic event, n, is determined from

$$\sum_{i=}^{n-}\sigma_i < \xi\sum_{i=}^{N}\sigma_i \le \sum_{i=}^{n}\sigma_i \ , \qquad (4.2)$$

[a] The term inelastic collision is a carryover from MCNP and means all reactions except elastic scattering and capture.

where ξ is a random number on the interval [0 to 1), N is the number of inelastic reactions, and the σ_i's are the inelastic reaction cross sections at the incident neutron energy.[2]

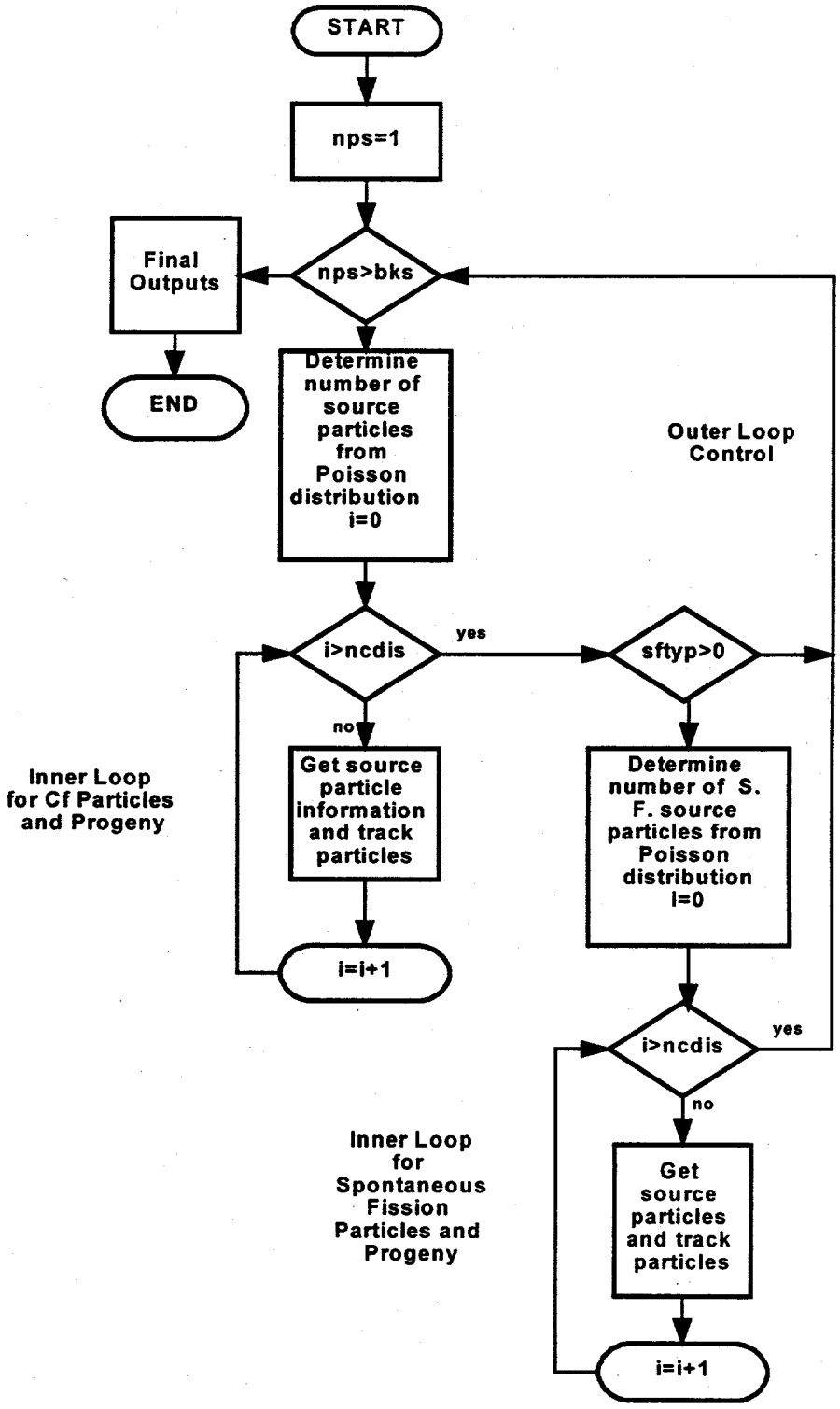

Figure 4.2. Structure of inner and outer loops

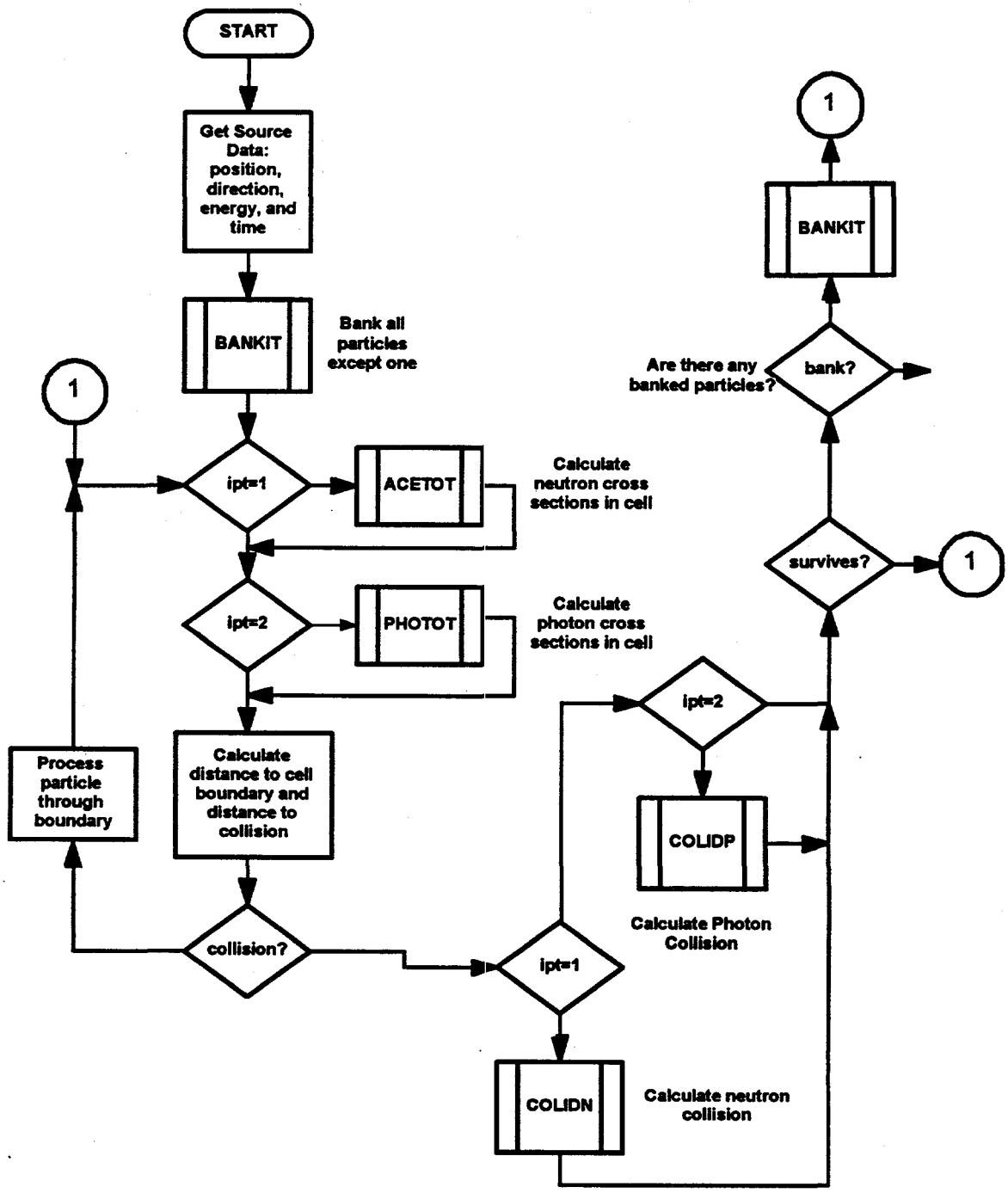

Figure 4.3. Particle tracking procedure

If the inelastic event is fission, the number of neutrons produced from fission is determined from Zucker and Holden's data or from Terrell's formula, depending on the fissioning isotope. The energy of the emerging neutrons is sampled from the appropriate spectrum indicated in the cross-section data file. The direction cosines may be either isotropic or determined from the experimental angular distribution data. Any neutrons produced from

fission are banked to be tracked later. If the particle is a gamma ray, the determination of the type of interaction is the same as that used for neutron collisions. However, the collision physics are different.[2] In the modified code the detailed physics treatment is used by default. The detailed physics treatment includes incoherent scattering, coherent scattering, the photoelectric effect, and pair production. Therefore, the total gamma ray cross section, σ_t, is

$$\sigma_t = \sigma_{ic} + \sigma_{co} + \sigma_{pe} + \sigma_{pp} , \tag{4.3}$$

where σ_{ic} is the incoherent scattering cross section, σ_{co} is the coherent scattering cross section, σ_{pe} is the photoelectric cross section, and σ_{pp} is the pair production cross section. The selection of the gamma ray event is determined in a manner similar to that of the neutron events.

The tracking and collision process is repeated for each particle until the particle either leaves the system or is absorbed by analog capture. Next, particles are retrieved from the bank, and the tracking process proceeds as before until all the source particles and their progeny have been tracked for the given data block. Then, the particles for the inherent fission source are tracked if the spontaneous fission source option is invoked. The inner loops are now complete for one data block, and the detector responses are then processed. After processing the detector responses, the outer loop variable is incremented, and the inner loop procedure is repeated. After the desired number of blocks have been calculated, the program calculates the final estimates of the APSDs and CPSDs and writes the data to a file.

5. INPUT AND OUTPUT EXAMPLES

To perform the MCNP-DSP calculations, the *idum* and *files* cards must be included in the MCNP input file. The *files* card is used to specify an extra file that contains data for the MCNP-DSP calculations and to specify the output file for MCNP-DSP. This chapter provides a listing of all of the options and their default values that can be used in the extra data file. This chapter also provides examples for the input and output files for the frequency domain, correlation domain, and pulsed neutron calculations.

5.1 EXTRA DATA FILE OPTIONS

The following is a description of the options that can be supplied in the extra data file to execute MCNP-DSP calculations. The options are specified with a unique 3 character identifier followed by an equal sign and an appropriate parameter. These options are similar to those found in the KENO-NR code and were chosen in this manner to minimize confusion when users switch from one code to the other.

The following options are required in each extra data file:

scd=x x is the number of source disintegrations per block and must be greater than one. The default value has been arbitrarily chosen as 32.

bks=x x is the number of blocks to calculate and must be an integer value greater than or equal to one. The default value has been arbitrarily chosen as 10000.

scx=x x is the source x-coordinate. There is no default variable for this parameter. The x-coordinate cannot coincide with a surface.

scy=y y is the source y-coordinate. There is no default variable for this parameter. The y-coordinate cannot coincide with a surface.

scz=z z is the source z-coordinate. There is no default variable for this parameter. The z-coordinate cannot coincide with a surface.

scc=x x is the source cell and must be an integer value. If the source cell is not specified, it will be determined using the source coordinates.

ntbn=x_1 x_2 x_1 is the number of time bins and must be a power of 2 no less than one and not greater than 1024. x_2 is the sampling rate and must be an integer greater than zero.

det=x_1..x_{12} There are 12 detector options that must be entered in the following order and must be entered regardless of the type of detector.

x_1 is the detector number. This entry must be an integer that begins with 2 and is labeled sequentially up to 5.

x_2 is the detector material. This entry must be also be an integer and coincide with a material in the input file.

x_3 is the detector type. The following are valid detector types:
$x_3 = 2$ for capture detectors;
$x_3 = 3$ for scattering detectors; and
$x_3 = 4$ for fission detectors.

x_4 is the lower neutron energy threshold and must be greater than zero and applies only to scatter detectors.

x_5 is the upper neutron energy threshold and must be greater than x_4 and applies only to scatter detectors.

x_6 is the lower photon energy threshold and must be greater than zero and applies only to scatter detectors.

x_7 is the upper photon energy threshold and must be greater than x_6 and applies only to scatter detectors.

x_8 is the pulse generation time. The pulse generation time is entered in nanoseconds and must be greater than zero. This parameter is only used with scatter detectors.

x_9 is the number of energy bins to bin the detector responses and only applies to scatter detectors.

x_{10} is the number of random neutron counts per data block.

x_{11} is the number of random photon counts per data block.

x_{12} is the detector efficiency for capture detectors. This entry must be entered regardless of the type of detector and is typically set equal to 1 for detectors other than capture detectors. This parameter is used to account for thresholds set in experiments when using ^{3}He detectors.

<u>At least two and no greater than four detectors must be specified for frequency domain or correlation domain calculations.
At least one and no greater than four detectors specified for pulsed neutron calculations.</u>

The following options are additional options that can be used in the calculations.

snu=x_1...x_{10} This parameter allows the user to change the default neutron emission distribution for the ^{252}Cf source. x_1 is the probability of 0 neutrons from ^{252}Cf, x_2 is the probability of 1 neutron from ^{252}Cf, x_3 is the probability of 2 neutrons from ^{252}Cf, and so forth, with a

maximum of 9 neutrons from ^{252}Cf.

spu=x_1...x_{21} This parameter allows the user to change the default photon emission distribution for the ^{252}Cf source. x_1 is the probability of 0 photons from ^{252}Cf, x_2 is the probability of 1 photon from ^{252}Cf, x_3 is the probability of 2 photons from ^{252}Cf, and so forth, with a maximum of 20 photons from ^{252}Cf.

cng=x This is the angular distribution option for the ^{252}Cf source. If x = 0, an isotropic distribution for neutrons from fission is used. If x = 1, the angular distribution for neutrons from fission is obtained from the Budtz-Jorgensen and Knitter data. x must be equal to zero or one.

ang=x This is the angular distribution option for neutron from fission. If x = 0, the default distribution for neutrons from fission obtained from cross-section data files. If x = 1, the angular distribution for neutrons from fission obtained from Budtz-Jorgensen and Knitter data x must be equal to zero or one.

stp=x This is the source type option. If x = 0, a ^{252}Cf source is used while a 14-MeV source is used if x = 1. x must be set equal to either zero or one and is equal to zero by default.

fil=x This is the parameter used to invoke the filter functions. If x = 0, the filter functions are not used. If x = 1, a Rockland filter is used in the calculations, and if x = 2, a Precision filter is used. The default is no filtering. This option is only valid for frequency domain calculations.

win=x This is the parameter to use the window functions. If x = 0, the window functions are not used. A Bartlett window corresponds to x = 1, a Hanning window corresponds to x = 2, and a Hamming window corresponds to x = 3. The default is no windowing. This option is only valid for frequency domain calculations.

smo=x This option allows the user to Hanning window the frequency spectra to smooth the frequency data. The choices for x are 'yes' and 'no,' with the default being 'no.' This option is valid only for frequency domain calculations.

rmf=x This option allows the user to remove the mean value from the detector time response prior to calculation of the frequency spectra or the correlation calculations. The choices for x are 'yes' and 'no,' with the default being 'no.'

bdr=x This option is used to treat the detector response as a binary signal. Only a one or a zero is allowed in the detector time bins and extra counts are ignored. This option should only be used for sampling rates near 1 GHz. The binary detector option is invoked if x = 1 and is ignored otherwise. This option is only valid for correlation domain calculations.

ltm=x This is the option used to perform the pulsed neutron calculations. The choices for x are 'yes' and 'no,' with 'no' being the default.

pro=x This option sets the processing mode for either frequency domain or correlation domain analyses. If x = 0, the standard frequency domain calculation is performed, and if x = 1, the correlation domain calculation is performed.

mod=x This option allows the user to use the shift register technique to calculate the correlation functions. This method may be faster for computing correlation functions for a few select problems. This option is invoked if x = 1 and is ignored otherwise. The default value for x is 0.

mlt=x This is the multiplicity option. This option is invoked if x = 1 and is ignored otherwise. If this option is used, an additional output file is created that contains integers that represent the number of times 0, 1, 2, etc., counts occurred in the data block for all detectors.

sfs=$x_1..x_j$ This option allows the user to specify the inherent fission source for one area in the cell. The number of parameters with this card depends on the cell type and the number of inherent fission sources.

x_1 is the number of inherent fission sources for the problem, and is limited to 5.

x_2 is the cell for the spontaneous fission source. If the cell is a part of an array, this parameter should be set equal to zero. The cell will then be determined from the spontaneous fission source coordinates.

x_3 is the spontaneous fission source volume type. The number of entries to describe this volume depends on the volume type. The following are valid geometry types:

$x_3 = 0$: volume bounded by six planes.

- x_0 x-coordinate of volume
- y_0 y-coordinate of volume
- z_0 z-coordinate of volume

z_0 z-coordinate of volume
x_p distance between x_0 and positive x-plane
x_m distance between x_0 and negative x-plane
y_p distance between y_0 and positive y-plane
y_m distance between y_0 and negative y-plane
z_p distance between z_0 and positive z-plane
z_m distance between z_0 and negative z-plane

$x_3 = 1$: volume is cylinder parallel to x-axis
x_0 x-coordinate of volume
y_0 y-coordinate of volume
z_0 z-coordinate of volume
r_i inner radius of cylinder
r_o outer radius of cylinder
x_p distance between x_0 and positive x-plane
x_m distance between x_0 and negative x-plane

$x_3 = 2$: volume is cylinder parallel to y-axis
x_0 x-coordinate of volume
y_0 y-coordinate of volume
z_0 z-coordinate of volume
r_i inner radius of cylinder
r_o outer radius of cylinder
y_p distance between y_0 and positive y-plane
y_m distance between y_0 and negative y-plane

$x_3 = 3$: volume is cylinder parallel to z-axis
x_0 x-coordinate of volume
y_0 y-coordinate of volume
z_0 z-coordinate of volume
r_i inner radius of cylinder
r_o outer radius of cylinder
z_p distance between z_0 and positive z-plane
z_m distance between z_0 and negative z-plane

$x_3 = 4$: volume is sphere
x_0 x-coordinate of volume
y_0 y-coordinate of volume
z_0 z-coordinate of volume
r_i inner radius of sphere
r_o outer radius of sphere

x_4 is the spontaneous fission source type.
$x_4 = 1$ ^{238}U, $x_4 = 2$ ^{240}Pu
$x_4 = 3$ ^{242}Pu, $x_4 = 4$ ^{242}Cm, $x_4 = 5$ ^{244}Cm

x_5 is the number of spontaneous fissions per block for spontaneous fission source x_4.

Entries 4 and 5 are supplied for each spontaneous fission source as determined by x_1.

5.2 FREQUENCY DOMAIN FILES

The following example problem consists of a 10.16-cm-high, 17.771-cm-OD, uranium metal cylinder with a ^{252}Cf source at its center. The uranium metal density is 18.76 g/cm^3 with 93.15 wt % ^{235}U, 5.64 wt % ^{238}U, 0.97 wt % ^{234}U, and 0.24 wt % ^{236}U. Two 7.62-cm-OD, 2.54-cm-long NE- 213 liquid scintillators are positioned on the radial surface of the cylinder. The MCNP input file is given in Fig. 5.1, and the extra data file contents for the frequency domain calculations are given in Fig. 5.2. Only an overview of the MCNP input file is presented. For a more detailed description of the MCNP input file consult ref. 12.

Description of Input File

Line 1: The first line of the input file is the title line.

Lines 2-11: These are comment cards used to describe the problem.

Lines 12-21: These are the cell description cards. The cell cards are used to describe the material's density and the surfaces that bound the particular cell.

Lines 26-49: These lines contain the surface description cards. For this simple problem the surfaces consist of planes and cylinders.

Lines 41-56: These are the data cards. Lines 45 through 51 describe the materials used in the calculations. Lines 54 through 56 are the control cards for this problem. The *prdmp* card on line 55 is used to control how often data are written to the MNCP-DSP output files. The *dbcn* card on line 56 is used to change the random number seed for the MCNP-DSP because the output data for several MCNP-DSP calculations are typically combined together.

Lines 60,61: These lines are used to execute the MCNP-DSP calculations. If the first entry on the *idum* card is 1, the MCNP-DSP calculation is executed and all other tallies will not be accumulated. The *files* card is used to specify two files. The first file contains the extra data parameters and is opened as a sequential, formatted file on unit 21. The second file is the MCNP-DSP output file. The output file is opened as a sequential formatted file on unit 22. Both files must be entered as sequential and formatted files. The record length is zero for sequential files.

```
1         i       i    10 16   i
2
3           i           93 15     235  5 64     238
4         0 97     234     0 24     236  18 76
5            235   235 0439
6            238   238 0508
7            234   234 0409
8            236   236 0456
9
10           6 022136736 10 23   v
11
12     1    1 0 048033    1   2   3                  i    1    i       i
13     2    0              1   2   3  10  11
14                         12  13                    i    1    i       i
15     3    2 0 088017    10  20  22                 i    1    i
16     4    3 0 088017    11  21  22                 i    1
17     6    0             10  20  12  13  22
18                          1   2                    i    1    i       i
19     7    0             11  21  12  13  22
20                          1   2                    i    1    i
21     8    0              1  2  20  21  12  13   i     0
22
23
24          i
25
26     1       0 0
27     2       10 16
28     3       8 8855
29
30     10   x   8 8856
31     11   x   8 8856
32     12       8 8856
33     13       8 8856
34
35
36
37     20   x   11 4256
38     21   x   11 4256
39     22    x  0 0   5 08   3 81
40
41
42
43          i
44
45      1   92235 50  0 932135  92238 50  0 055726
46            92234 50  0 009748  92236 50  0 002391
47
48          213 i i   i i
49
50      2   1001 50   0 5481  6012 50  0 4519
51      3   1001 50   0 5481  6012 50  0 4519
52
53
54
55          1  300
56          19333486327999 11  725525
57
58
59
60     i    1
61      i   21   10 x    0 22   10 1    0
```

Figure 5.1. MCNP uranium metal cylinder example input file

```
1.  scd=32
2.  bks=5000
3.  scx=0.0
4.  scy=0.0
5.  scz=5.08
6.  tbn=1024  10000000.
7.  det=2 2 3 0.3 50.0 0.3 50.3 2.0 0 0 0 1.
8.  det=3 3 3 0.3 50.0 0.3 50.3 2.0 0 0 0 1.
9.  stp=0
10. cng=0
11. end
```

Figure 5.2. MCNP-DSP extra data file for frequency domain calculations

Description of Extra Data File

Line 1: There are 32 source disintegrations per block (*scd*) in this example.

Line 2: The number of blocks to calculate (*bks*) is 5000.

Lines 3-5: These lines represent the coordinates of the source.

Line 6: This line specifies the number of time channels as 1024 with a sampling rate of 10 MHz.

Lines 7-8: These lines describe the detectors in the problem. The source is detector 1 and does not need to be labeled. This problem has two detectors, 2 and 3. Both detectors are scattering detectors. The lower and upper neutron thresholds are 0.3 MeV and 50.0 MeV, respectively. The lower and upper gamma ray thresholds are 0.3 and 50.3 MeV respectively. Typically, the neutron threshold is set higher than that for the gamma ray. The pulse generation time is set to 2 ns. There are no energy bins in this calculation and there are no neutron or gamma ray background counts for the detector. The last parameter only pertains to capture detectors; therefore, it is set equal to one for scattering or fission detectors. **For the frequency domain calculations, at least two detectors (2 and 3) must be listed in the extra data file**.

Line 9: This line specifies that the source type is ^{252}Cf and could have been omitted.

Line 10: The *cng* option is used to determine the direction sampling for the ^{252}Cf source. This option could have been omitted because the default value is zero.

Line 11: The *end* parameter is used to specify the end of the extra file. This option could have also been omitted.

There are two or more output files from the frequency domain MCNP-DSP calculations. The first contains general information on the number of counts for each detector and is specified in the MCNP input file. The second output file(s) contains the frequency spectra for the detectors. If the problem is a combined neutron-photon calculation as in the example, there will be three files created that contain the APSDs and CPSDs for the detectors for the neutron response, the gamma response, and the combined neutron and gamma ray response. The general output filename as specified in Fig. 5.1 is *um10f.1*. Three additional files will contain the APSDs and CPSDs. These are *um10f.1.123.fft.n*, *um10f.1.123.fft.p*, and *um10f.1.123.fft.np*, where the first file contains the spectra for the neutron response, the second file contains the spectra for the gamma response, and the third file contains the spectra for the combined neutron and gamma ray response as indicated by the last extension. The other filename extensions have distinct meanings. The first part that has the '*123*' indicates that this file contains the frequency spectra for the APSDs of detectors #1, #2, and #3, and the CPSDs between 1 and 2, 1 and 3, and 2 and 3. The '*fft*' indicates that the file contains data that have been Fourier transformed. The output files for the frequency domain calculation are presented in Figs. 5.3 and 5.4. The frequency spectra for multiple runs can be combined by combining the APSDs and CPSDs based on the number of blocks of data accumulated. If the user combines the frequency spectra from several runs, the Monte Carlo calculation for each run must begin with a separate random number seed that can be specified using the *dbcn* card in the MCNP input file.

The MCNP-DSP output file begins with a description of the source used for the calculations. The average number of source events per data block and the number of data blocks accumulated are printed. The source cell and coordinate positions are also given. Next, the detector options used in the calculation are given. After the detector options are listed, the neutron tracking information is provided for all neutrons and for the source neutrons. The number of fissions, captures, and (n,xn) reactions and the number of leakages are tallied for all neutrons and tallied separately for source neutrons. The average number of neutrons from the source and system fissions are estimated along with the Diven factor for both source and system neutrons. The average energy of neutrons from the source fission and from system fissions is also calculated. After these parameters, the total number of neutron detections is given for the number of blocks specified at the beginning of the output file. The number of detections due to directly counting source particles is also listed. Information similar to that for the neutrons is also provided for the gamma rays.

****

* Source Information *

****

Number of Source Events/ Data Block= 31.91
Number of Data Blocks= 5000
Source Cell= 0
Source Surface= 0
Source Coordinates
Source X-Coordinate= 0.0000
Source Y-Coordinate= 0.0000
Source Z-Coordinate= 5.0800

****

****

* Detector Information *

****

Detector Id.	Mat	Type	Neutron Low.	Neutron Up.	Photon Low.	Photon Up.	Gen. Time (ns)
2	2	3	0.30000	50.00000	0.30000	50.30000	2.00000
3	3	3	0.30000	50.00000	0.30000	50.30000	2.00000

****

****

* Neutron Tracking Information *

****

Neutrons Followed: 13006109
Number of Fissions: 4751262
Number of Captures: 523259
Number of (n,xn): 22966
Number of Leakages: 7708622
Src Neutrons Followed: 602239
Number of Fissions (Sc) 285935
Number of Captures (Sc) 31608
Number of (n,xn) (Sc) 1642
Number of Leakages (Sc) 283054
S.F. Neutrons Followed: 0

****

* Calculated Parameters *

****

Average Sc Nu-Bar: 3.77456 +/- 0.00001
Average Sc Nu-Sq-Bar: 15.82917
Source Diven Factor: 0.84610
Average Sc Energy (MeV) 2.1269 +/- 0.00000
Average Nu-Bar: 2.60097 +/- 0.00000
Average Nu-Sq-Bar: 8.09311
Diven Factor: 0.81184
Average Energy (MeV) 2.0377 +/- 0.00000

****

* Detector Information *

****

Det. Id.	Det. Mat	Det. Type	No. Detects	No. Sc Detects
2	2	3	98317	2522
3	3	3	98510	2604

Figure 5.3. MCNP-DSP output file

```
**************************************************************
*                    Photon Tracking Information             *
**************************************************************
      Photons Followed:                        76102080
      Number of Captures:                      73998563
      Number of Pair Productions                 962610
      Number of Leakages:                       1140907
      Sc Photons Followed:                      1244603
      Number of Captures (Sc)                   1201154
      Number of Pair Productions (Sc)             41896
      Number of Leakages (Sc)                      1553
**************************************************************
*                    Calculated Parameters                   *
**************************************************************
      Average Sc G-Bar:                 7.80061 +/- 0.00002
      Average Sc G-Sq-Bar:              70.773170
      Source Photon Diven Factor:       1.03489
      Average Sc Energy (MeV)           0.8974 +/- 0.00000
**************************************************************
*                    Detector Information                    *
**************************************************************
Det. Id.   Det. Mat   Det. Type   No. Detects   No. Sc Detects
   2          2          3          4703             3
   3          3          3          4715             1
```

Figure 5.3. (continued)

The frequency domain output files contain the APSDs and the CPSDs. The entries in these files is as follows: APSD of the source, APSDs of the detectors, the real part of the CPSD between the source and detector 2, the imaginary part of the CPSD between the source and detector 2, the real part of the CPSD between the source and detector 3, the imaginary part of the CPSD between the source and detector 3, the real part of the CPSD between detectors, and the imaginary part of the CPSD between detectors. Each section is divided by a header that contains the following information: the parameter name, the frequency interval, the Nyquist frequency, the number of blocks, and the number of points for each spectra. The frequency dependent spectra are written out in a 6-column format and read across row by row. The first entry in column 1 is the spectra value at zero frequency; the first entry in column 2 is the spectra value at 1 times the frequency interval; the first entry in column 3 is the spectra value at 2 times the frequency interval, etc. In the example shown in Fig. 5.4, the sampling interval is 9765.6 Hz, the Nyquist frequency is 5 MHz, the number of blocks is 5000, and the number of points for each spectra is 512. When plotting the frequency spectra, the spectra value at zero frequency is ignored. Only the frequency spectra for the neutron response is shown in Fig. 5.4; there would be a similar file for the spectra for the gamma ray response and for the combined neutron and gamma ray response.

```
    psd #11  0.97656E+04  0.50000E+07  0.50000E+04 512
 0.105015E+04 0.314440E+02 0.313886E+02 0.324211E+02 0.315791E+02 0.314126E+02
(skip 84 lines)
0.314724E+02  0.317303E+02
    psd #22  0.97656E+04  0.50000E+07  0.50000E+04 512
 0.487841E+03 0.979250E+02 0.100738E+03 0.990213E+02 0.983378E+02 0.992246E+02
 (skip 84 lines)
0.377028E+02  0.372380E+02
    psd #33  0.97656E+04  0.50000E+07  0.50000E+04 512
 0.491389E+03 0.100433E+03 0.102049E+03 0.100609E+03 0.100482E+03 0.100902E+03
 (skip 84 lines)
 0.376337E+02 0.381704E+02
   rcpsd #12  0.97656E+04  0.50000E+07  0.50000E+04 512
 0.647746E+03 0.186477E+02 0.192486E+02 0.196353E+02 0.200935E+02 0.187655E+02
(skip 84 lines)
0.121656E+01  0.226474E+01
   icpsd #12  0.97656E+04  0.50000E+07  0.50000E+04 512
 0.000000E+00 -0.835362E+00 -0.181380E+00 -0.370003E+00 -0.267435E+00 -0.797343E+00
(skip 84 lines)
-0.614186E-01 -0.747087E+00
   rcpsd #13  0.97656E+04  0.50000E+07  0.50000E+04 512
 0.648219E+03 0.191366E+02 0.192945E+02 0.196272E+02 0.197184E+02 0.188626E+02
(skip 84 lines)
 0.185097E+01 0.199959E+01
   icpsd #13  0.97656E+04  0.50000E+07  0.50000E+04 512
 0.000000E+00 -0.118515E+00 -0.827517E-01 0.169828E+00 -0.709216E+00 -0.826886E+00
(skip 84 lines)
-0.840099E+00 -0.251599E+00
    rcpsd #23  0.97656E+04  0.50000E+07  0.50000E+04 512
 0.459494E+03 0.688133E+02 0.711327E+02 0.697201E+02 0.695946E+02 0.703965E+02
 (skip 84 lines)
 0.979691E+01 0.103884E+02
    icpsd #23  0.97656E+04  0.50000E+07  0.50000E+04 512
 0.000000E+00 0.999937E+00 0.183756E+00 0.399826E+00 0.527544E+00 0.279180E+00
(skip 84 lines)
-0.443189E-01  0.370622E-01
```

Figure 5.4 Partial listing of MCNP-DSP frequency domain FFT file

5.3 CORRELATION DOMAIN FILES

The correlation domain calculation is very similar to the frequency domain calculations. The difference is that correlation functions are calculated and the circular correlation functions are Fourier transformed when the particle tracking is completed to obtain the frequency spectra. The extra data file should contain the option *pro=1* to execute the correlation calculation. There are additional output files created when using this option that contain the linear unbiased correlation functions. For the example problem given in Fig. 5.1, the extra files would be *um10f.1.123.cor.n*, *um10f.1.123.cor.p*, and *um10f.1.123.cor.np*. The first file contains the spectra for the neutron response, the second file contains the spectra for the gamma response, and the third file contains the spectra for the combined neutron and gamma ray response, as indicated by the last extension. The filename extensions have distinct meanings. The first part that has the '*123*' indicates that this file contains the autocorrelation of detectors 1, 2, and 3, and the cross correlations between 1 and 2, 1 and 3, and 2 and 3. The '*cor*' extensions indicate that the file contains correlation functions. Because the autocorrelation functions are symmetric, only their positive lags are written to file. The cross correlations are written for positive and negative lags. There is a header that separates the correlation functions in the output file. The header contains the following information: the parameter name, the total period of the data block, the total number of counts for the detector, and the number of blocks. An abbreviated listing of the correlation output file is given in Fig. 5.5. For the example given in Fig. 5.5, the measurement period per block is 1024 ms, and the number of blocks is 5000. The cross correlation between the source and the detectors can be compared with the time distribution of counts after ^{252}Cf fission from the pulsed neutron calculations. As in the frequency domain calculations, at least two detectors (2 and 3) must be specified in the extra data file. The correlation spectra or the frequency spectra can also be combined, as previously described in Sect. 5.2.

```
 autocorrelate11  .10240E-03  .15955E+06          5000
    0       0.160621093750000E+03
    1       0.492277614858260E+01
    (skip 1021 lines)
 1023       0.400000000000000E+01
autocorrelate22  .10240E-03  .98374E+05          5000
    0       0.302697265625000E+03
    1       0.736559139784946E+02
    (skip 1021 lines)
 1023       0.000000000000000E+00
autocorrelate33  .10240E-03  .98540E+05          5000
    0       0.306005859375000E+03
    1       0.750283479960899E+02
    (skip 1021 lines)
 1023       0.000000000000000E+00
crosscorrelate12  .102400000000000E-03
    (skip 1020 lines)
    -3      0.295592556317336E+01
    -2      0.302446183953033E+01
    -1      0.303616813294233E+01
    0       0.459257812500000E+02
    1       0.437086999022483E+02
    2       0.118248532289628E+02
    3       0.508423114593536E+01
   (skip 1020 lines)
crosscorrelate13  .102400000000000E-03
   (skip 1020 lines)
    -3      0.295396669931440E+01
    -2      0.308121330724070E+01
    -1      0.306744868035191E+01
    0       0.462705078125000E+02
    1       0.432707722385142E+02
    2       0.121908023483366E+02
    3       0.496180215475025E+01
    (skip 1020 lines)
crosscorrelate23  .102400000000000E-03
    (skip 1020 lines)
    -3      0.569735553379040E+01
    -2      0.178767123287671E+02
    -1      0.716510263929619E+02
    0       0.164506835937500E+03
    1       0.711055718475073E+02
    2       0.176223091976517E+02
    3       0.578942213516161E+01
    (skip 1020 lines)
```

Figure 5.5. Partial listing of MCNP-DSP correlation domain COR file

5.4 PULSED NEUTRON FILES

The example for the pulsed neutron calculation is very simple and is a 5.08-cm-diam, 2.54-cm-long, NE-213 liquid scintillator spaced 0.25 m from a ^{252}Cf source. A listing of the input file is given in Fig. 5.6. As in the example given in Sect. 5.2, the parameters *idum* and *files* are used to implement the MCNP-DSP calculations. The extra data file for the pulsed neutron calculation is the same as that for the frequency domain calculation with a few exceptions. The extra data file for this example is shown in Fig. 5.7. When performing pulsed neutron calculations, *scd* is treated as the total number of ^{252}Cf source fissions, and *bks* must be equal to one. **Because of the manner in which the pulsed neutron measurement executes, all data will be lost if it is interrupted as can be done with standard MCNP**. The user is warned to select a reasonable value for *scd* and to combine the detector responses for several runs. If several runs are combined, the user must start each run with a different random number seed using the *dbcn* card in the MCNP input file, as shown in Fig. 5.6. Unlike the frequency domain or correlation domain calculations, one detector can be used in the pulsed neutron calculations. In the example given in Fig. 5.6, the summary output file *detex.1* and the detector time response file *detex.1.tim* will be created.

```
Source and detector in air: 0.25 m
c
c   NE-213 Detector in Air
1   1 0.088017 +1   -2 -10 imp:n,p=1
2   0           +2 -20 -10 imp:n,p=1
3   0            -1:+20:+10 imp:n,p=0

c
c   Detector Planes
c   ===============
1   px  0.0
2   px  2.54
c
10  cx  2.54
c
c
c   Source Void
c   ===========
20  px  27.55

mode n p
 m1    1001.50c  0.5477  6012.50c 0.4523
prdmp 1j -30
dbcn   19333486379999 11j 725525
idum   1
files  21 detex.x s f 0 22 detex.1 s f 0
```

Figure 5.6. MCNP-DSP source-detector pulsed neutron input file

```
1.    scd=500000.
2.    bks=1
3.    scx=27.54
4.    scy=0.0
5.    scz=0.0
6.    ltm=yes
7.    tbn=512  1000000000.
8.    det=2 1 3 0.3 50.0 0.3 50.3 2.0 0 0 0 1.
9.    stp=0
10.   cng=0
11.   end
```

Figure 5.7 MCNP-DSP extra data file for pulsed neutron calculations

Description of Extra Data File

Line 1: The total number of source disintegrations for this run is 500,000. The actual total number of source disintegrations will be sampled from a Poisson distribution with mean value 500,000. The user must refer to the summary output file for the actual total number of source disintegrations that were simulated.

Line 2: This is the number of blocks to run and **must** be equal to one. Otherwise, the user could fill up his disk because the detector time responses will be appended to the '*tim*' files.

Lines 3-5: As in the previous example, these are the source coordinates. The source cell is not specified but will be determined from the source position.

Line 6: This option is used to execute the pulsed neutron contribution.

Line 7: This line specifies the number of time channels as 512 with a sampling rate of 1 GHz.

Line 8: This line describes the detectors in the problem. The source is detector 1 and does not need to be labeled. This problem has one scattering detector 2. The lower and upper neutron thresholds are 0.3 MeV and 50.0 MeV respectively. The lower and upper gamma ray thresholds are 0.3 and 50.3 MeV respectively. Typically, the neutron threshold is set higher than that for the gamma ray. The pulse generation time is set to 2 ns. There are no energy bins in this calculation, and there are no neutron or gamma ray background counts for the detector. The last parameter pertains only to capture detectors; therefore, it is set equal to one for scattering or fission detectors. In the pulsed neutron calculations, the user can input one to four detectors.

Line 9: This line specifies that the source type is ^{252}Cf and could have been omitted.

Line 10: The *cng* option is used to determine the direction sampling for the ^{252}Cf source. This option could have been omitted because the default value is zero.

Line 11: The *end* parameter is used to specify the end of the extra file. This option could have also been omitted.

The information in the summary output file for this problem is similar to the one given in the previous example. An abbreviated listing of the time response output file is given in Fig. 5.8. This file contains the total detector time response for the source and the detectors. The detector time responses are separated by a header that describes the particle type and the detector number. The user should note that the source time response is only in the first time bin. This results because all source events start at time zero. The neutron, photon, and combined neutron and photon time response for the source is the same because this is the actual number of source events and not the number of source particles. The user should also note that the number of source events for the example problem is not exactly 500,000 but is 500,374 because this number is sampled from a Poisson distribution. The source time response is followed by the detector time response for neutron, gamma rays, and then the combined response. The detector time response is written in ten columns. Columns 2, 4, 6, 8, and 10 contain zeros and can be ignored. These columns are zero because of the manner in which the time response array is written. The time bins are read across: the first entry in column 1 corresponds to the first time bin, the first entry in column 3 corresponds to the second time bin, the first entry in column 5 corresponds to the third time bin, the first entry in column 7 corresponds to the fourth time bin, the first entry in column 9 corresponds to the fifth time bin, the second entry in column one corresponds to the sixth time bin, and so forth. The width of the time bin is determined by the inverse of the sampling rate and would be 1 ns for this example problem. When the data are plotted, the time of detection is typically taken as the midpoint of the time bins. The pulsed neutron spectra are typically represented in the form counts per source event per time interval. This is useful for comparing calculations in which different number of source sizes or different sampling rates were used.

```
Neutron Time Response for Detector # 1
500374.    0.    0.    0.    0.    0.    0.    0.    0.    0.
     0.    0.    0.    0.    0.    0.    0.    0.    0.    0.
(skip 101 lines)
Photon Time Response for Detector # 1
500374.    0.    0.    0.    0.    0.    0.    0.    0.    0.
     0.    0.    0.    0.    0.    0.    0.    0.    0.    0.
 (skip 101 lines)
Neutron and Photon Time Response for Detector # 1
500374.    0.    0.    0.    0.    0.    0.    0.    0.    0.
     0.    0.    0.    0.    0.    0.    0.    0.    0.    0.
(skip 101 lines)
Neutron Time Response for Detector # 2
     0.    0.    0.    0.    0.    0.    0.    0.    0.    0.
     1.    0.   10.    0.   17.    0.   56.    0.   82.    0.
   117.    0.  114.    0.  104.    0.   84.    0.   91.    0.
    74.    0.   64.    0.   69.    0.   55.    0.   46.    0.
    35.    0.   50.    0.   39.    0.   30.    0.   23.    0.
    27.    0.   18.    0.   14.    0.   13.    0.    5.    0.
     9.    0.    7.    0.    9.    0.    4.    0.    3.    0.
     5.    0.    1.    0.    0.    0.    0.    0.    0.    0.
     1.    0.    0.    0.    1.    0.    0.    0.    0.    0.
     0.    0.    0.    0.    1.    0.    0.    0.    0.    0.
     0.    0.    0.    0.    0.    0.    0.    0.    0.    0.
(skip  92 lines)
Photon Time Response for Detector # 2
   419.    0.    2.    0.    0.    0.    0.    0.    0.    0.
     0.    0.    1.    0.    0.    0.    0.    0.    0.    0.
     0.    0.    0.    0.    0.    0.    0.    0.    0.    0.
     0.    0.    0.    0.    0.    0.    0.    0.    0.    0.
(skip 99 lines)
Neutron and Photon Time Response for Detector # 2
   419.    0.    2.    0.    0.    0.    0.    0.    0.    0.
     1.    0.   11.    0.   17.    0.   56.    0.   82.    0.
   117.    0.  114.    0.  104.    0.   84.    0.   91.    0.
    74.    0.   64.    0.   69.    0.   55.    0.   46.    0.
    35.    0.   50.    0.   39.    0.   30.    0.   23.    0.
    27.    0.   18.    0.   14.    0.   13.    0.    5.    0.
     9.    0.    7.    0.    9.    0.    4.    0.    3.    0.
     5.    0.    1.    0.    0.    0.    0.    0.    0.    0.
     1.    0.    0.    0.    1.    0.    0.    0.    0.    0.
     0.    0.    0.    0.    1.    0.    0.    0.    0.    0.
     0.    0.    0.    0.    0.    0.    0.    0.    0.    0.
 (92 lines deleted)
```

Figure 5.8 Partial listing of MCNP-DSP pulsed neutron time file

APPENDIX A
SPONTANEOUS FISSION DISTRIBUTIONS

APPENDIX A. SPONTANEOUS FISSION DISTRIBUTIONS

The P(ν) data for ^{252}Cf was obtained from Spencer's measured data and are listed in Table A.1. The P(ν) data for ^{238}U, ^{240}Pu, ^{242}Pu, ^{242}Cm, and ^{244}Cm were obtained from Zucker and Holden's tabulated data and are listed in Tables A.2 to A.6.

Table A.1. P(ν) probabilities for ^{252}Cf

ν	P(ν)
0	0.00211
1	0.02467
2	0.12290
3	0.27144
4	0.30763
5	0.18770
6	0.06770
7	0.01406
8	0.00167
9	0.00010

Table A.2. P(ν) probabilities for ^{238}U

ν	P(ν)
0	0.0481677
1	0.2485215
2	0.4253044
3	0.2284094
4	0.0423438
5	0.0072533

Table A.3. P(ν) probabilities for ^{240}Pu

ν	P(ν)
0	0.0631852
1	0.2319644
2	0.3333230
3	0.2528207
4	0.0986461
5	0.0180199
6	0.0020406

Table A.4. P(ν) probabilities for ^{242}Pu

ν	P(ν)
0	0.0679423
1	0.2293159
2	0.3341228
3	0.2475507
4	0.0996922
5	0.0182398
6	0.0031364

Table A.5. P(ν) probabilities for ^{242}Cm

ν	P(ν)
0	0.0212550
1	0.1467407
2	0.3267531
3	0.3268277
4	0.1375090
5	0.0373815
6	0.0025912
7	0.0007551
8	0.0001867

Table A.6. P(ν) probabilities for ^{244}Cm

ν	P(ν)
0	0.0150050
1	0.1161725
2	0.2998427
3	0.3331614
4	0.1837748
5	0.0429780
6	0.0087914
7	0.0002744

APPENDIX B
SPONTANEOUS FISSION NEUTRON ENERGY SPECTRA

APPENDIX B. SPONTANEOUS FISSION NEUTRON ENERGY SPECTRA

The energy spectra of neutrons from spontaneous fission can be represented with a Maxwellian or a Watt spectrum. The prompt neutron energy spectrum, *N(E)*, represented by the Maxwellian spectrum is

$$N(E) = \frac{2}{\sqrt{\pi}} \frac{\sqrt{E}}{T^{3/2}} e^{-E/T} , \tag{B.1}$$

where E is the energy on the neutron and T is the nuclear temperature. The nuclear temperature is typically 1.42 MeV for ^{252}Cf. The Maxwellian does not agree precisely with the measured spectrum for ^{252}Cf; therefore, Mannhart[17] developed an energy dependent correction factor, *R(E)*, which when multiplied by the Maxwellian spectrum would reproduce the measured spectrum. A least-squares polynomial regression model was used to obtain a functional form for Mannhart's correction factor. For energies less than 5 MeV, the correction factor is represented by

$$R(E) = 0.955 + 0.707E - 0.04E^2 + 0.02E^3 - 0.00451E^4 + 0.000368E^5 . \tag{B.2}$$

For energies greater than 5 MeV, the correction factor is represented as

$$R(E) = 1.16 - 0.432E + 0.00185E^2 - 0.0000316E^3 . \tag{B.3}$$

The energy ranges were chosen such that the functional representation adequately reproduces Mannhart's discrete points. Other fits could be applied to Mannhart's correction factor that when multiplied by the Maxwellian should adequately reproduce the measured spectra. The average neutron energy obtained from the corrected spectrum is 2.13 MeV, which agrees well with the measured value. The integral of the corrected spectrum as a function of energy was normalized to unity. A least-squares polynomial regression was used to fit the energy as a function of the normalized integral, that is, making the energy a polynomial function of the random variable.

The energy spectra of the inherent spontaneous fission sources is represented by the Watt spectrum,

$$N(E) = Ce^{-E/a} \sinh(bE)^{1/2}, \tag{B.4}$$

where E is the neutron energy, C is a normalization constant, and a and b are the parameters for the Watt spectrum. Some of the Watt parameters for the inherent spontaneous fission sources can be found in the MCNP manual, and others were supplied by David Madland of Los Alamos National Laboratory. A listing of the Watt parameters for the inherent spontaneous fission sources is presented in Table B.1.

Table B.1. Watt parameters for inherent spontaneous fission sources

Isotope	a (MeV)	b (MeV^{-1})
^{238}U	0.78	5.194
^{240}Pu	0.799	4.903
^{242}Pu	0.834	4.432
^{242}Cm	0.891	4.046
^{244}Cm	0.906	3.848

REFERENCES

1. T. E. Valentine and J. T. Mihalczo, "MNCP-DSP: A Neutron and Gamma Ray Monte Carlo Calculation of Source-Driven Noise-Measured Parameters," *Ann. Nucl. Eng.* **23** 16 1271 (1996).

2. J. F. Briesmeister, ed., *MCNP4A-A General Monte Carlo N-Particle Transport Code*, La-12625-M, Los Alamos National Laboratory, 1993.

3. V. K. Paré and J. T Mihalczo, "Reactivity from Power Spectral Density Measurements with Californium-252," *Nucl. Sci. Eng.* **56**, 213 (1975).

4. J. T. Mihalczo and V. K. Paré, "Nuclear Weapons Identification System (NWIS)," *Arms Control and Nonproliferation Technologies*, Report on Nuclear Warhead Dismantlement, DOE/AN/ANCI-94C, Lawrence Livermore National Laboratory, Third Quarter 1994.

5. T. E. Valentine and J. T. Mihalczo, "Enrichment of Uranium Metal from NWIS Signatures," *Proc. Of the 36th Annual Meeting of Institute. of Nuclear Materials Management*, Palm Desert, California, 1995.

6. J. T. Mihalczo and W. T. King, "Quality Assurance Verification of High-Flux Isotope Reactor Fuel Elements by the ^{252}Cf-Source-Drivne Noise Analysis Method," *Nucl. Technol.* **84**, 205 (1989).

7. J. T. Mihalczo, "Use of Noise Analysis Methods in Process Monitoring in Future Fuel Cycles," *Proc. Of Global '93 Future Nuclear Systems: Emerging Fuel Cycles and Waste Disposal Options*, Seattle, Washington, Vol. 1, September (1993).

8. T. E. Valentine and J. T. Mihalczo, "MCNP-DSP Calculations of the ^{252}Cf-Source-Driven Noise Analysis Measurements of High-Enriched Uranium Metal Cylinders," *Proc. Of 5th International Conference on Nuclear Criticality Safety*, Albuquerque, New Mexico, 1995.

9. E. P. Ficaro, *KENO-NR: A Monte Carlo Code Simulating the ^{252}Cf-Source-Driven Noise Analysis Experimental Method for Determining Subcriticality*, Ph.D. Dissertation, University of Michigan, 1991.

10. L. M. Petrie, and N. F. Landers, "KENO V.a: An Improved Monte Carlo Criticality Program with Supergrouping," ORNL/NUREG/CSD-2, Oak Ridge National Laboratory, 1984.

11. J. Terrel, *Phys. Rev.* **113**, 527 (1959).

12. M. S. Zucker, and N. E. Holden, "Energy Dependence of Neutron Multiplicity P_ν in Fast-Neutron-Induced Fission for $^{235,238}U$ and ^{239}Pu," BNL-38491, 1986.

13. R. R. Spencer, R. Gwin, R. and Ingle, "A Measurement of the Average Number of Prompt Neutrons from Spontaneous Fission of Californium-252," *Nucl. Sci. Eng.* **80**, 603 (1982).

14. N. E. Holden and M. S. Zucker, "A Reevaluation of the Average Prompt Neutron Emission Multiplicity (Nubar) Values from Fission of Uranium and Transuranium Nuclides," BNL-NCS-35513, Brookhaven National Laboratory.

15. C. Budtz-Jorgensen and H. H. Knitter, "Simultaneous Investigation of Fission Fragments and Neutrons in ^{252}Cf (SF)," *Nucl. Phy.* **A490**, 307 (1988).

16. J. R. Nix, Los Alamos National Laboratory, personal communication 1994.

17. W. Mannhart, "Evaluation of the Cf-252 Fission Neutron Spectrum Between 0 MeV and 20 MeV," *Proc. Advisory Group Mtg. Neutron Sources,* Leningrad, USSR, 1986 (IAEA-TECDOC-410), Vienna, 1987.

18. R. Seamon, Los Alamos National Laboratory, personal communication 1994.

19. R. Vandenbosch and J. R. Huizenga, *Nuclear Fission*, Academic Press, New York, 1973.

20. G. S. Brunson, Jr., *Multiplicity and Correlated Energy of Gamma Rays Emitted in the Spontaneous Fission of Californium-252*, Ph.D. Thesis, Univ. of Utah, 1982.

21. C. Wagemans, *The Nuclear Fission Process*, CRC Press, Inc., Boca Raton, Florida, 1991.

22. F. C. Maienschein, R. W. Peelle, T. A. and Love, *Neutron Phys. Ann. Prog. Rep. For Sept. 1, 1958*, ORNL-2609, Oak Ridge National Laboratory.

23. H. Goldstein, *Fundamental Aspects of Reactor Shielding*, Addison-Wesley Publishing Company, Inc., Reading, Massachusetts, 1959.

24. H. Nifenecker, C. Signarbieux, M. Ribrag, J. Poitou, and J. Matuszek, "Gamma-Neutron Competition in the De-excitation Mechanism of the Fission Fragments of ^{252}Cf," *Nucl. Phys.* **A189**, 209 (1972).

25. A. V. Oppenheim and R. W. Schafer, *Discrete-Time Signal Processing*, Prentice-Hall Inc., Englewood Cliffs, New Jersey, 1989.

INTERNAL DISTRIBUTION

1-10. T. E. Valentine
11. R. G. Gilliland
12. C. M. Hopper
13. L. C. Leal
14. J. A. March-Leuba
15. J. K. Mattingly
16. D. W. McDonald
17. J. T. Mihalczo
18. G. N. Miller
19. J. P. Renier
20. F. J. Schultz
21. T. Uckan
22. R. E. Uhrig
23. R. M. Westfall
24. B. A. Worley
25. M. C. Wright
26. M. S. Wyatt
27. Central Research Library
28. Y-12 Technical Reference Section
29. Laboratory Records–Record Copy
30. I &C Division Publications Office

EXTERNAL DISTRIBUTION

31. Mark E. Abhold, Los Alamos National Laboratory, P.O. Box 1663, NIS-5, MS E540, Los Alamos, NM 87545
32. Steven E. Aumeier, Argonne National Laboratory, P.O. Box 2528, Idaho Falls, ID 83403
33. G. K. Becker, Idaho National Engineering Lab, P.O. Box 1625, MS-2114, Idaho Falls, ID 83415
34. C. L. Bendixsen, Idaho National Engineering Lab, P.O. Box 1625, MS-3140, Idaho Falls, ID 83415
35. Ron Brodzinski, Pacific North National Lab, Battele Blvd., P.O. Box 999, MS-P801, Richland, Washington 99352
36. Ken Bulmahn,, 283 Springwood Lane, Idaho Falls, Idaho 83404-8104
37. David Burke, Westinghouse Savannah River Corp., 707C, Room 306, Aiken, SC 29808
38. Jerry Cole, Idaho National Engineering Lab, P.O. Box 1625, MS-2114, Idaho Falls, ID 83415
39. M. A. Ebner, Idaho National Engineering Lab, P.O. Box 1625, MS-3114, Idaho Falls, ID 83415
40. B. Einziger, Pacific North National Lab, Battele Blvd., P.O. Box 999, MS-K245, Richland, Washington 99352
41. R. I. Ewing, Sandia National Laboratory, P.O. Box 5800, MS-0716, Albuquerque, NM 87185-0716
42. R. A. Forster, Los Alamos National Laboratory, P.O. Box 1663, X-TM, MS B226, Los Alamos, NM 87545
43. Larry B. Foulke, Westinghouse Electric Corp., Bettis Atomic Power Laboratory, P.O. Box 79, West Mifflin, PA 15122-0079

44. Victor Gavron, Los Alamos National Laboratory, P.O. Box 1663, NIS-5, MS-E540, Los Alamos, NM 87545
45. Thomas B. Gosnell, Lawrence Livermore National Laboratory, 7000 East Avenue, L-175, Livermore, California 94550
46. D. L. Hale, Idaho National Engineering Lab, P.O. Box 1625, MS-3765, Idaho Falls, ID 83415
47. Jim Howell, Westinghouse Savannah River Corp., 773-41A, Room 134, Aiken, SC 29808
48. B. Howard, Westinghouse Savannah River Corp., 730A, Room 191, Aiken, SC 29808
49. Sin-Tao Hsue, Los Alamos National Laboratory, P.O. Box 1663, NIS-5, MS-E540, Los Alamos, NM 87545
50. Natraj Iyer, Westinghouse Savannah River Corp., 773A, Room 134, Aiken, SC 29808
51. Marc Loibel, Westinghouse Savannah River Corp., 730A, Room 190, Aiken, SC 29808
52. P. M. Lovett, Department of Energy Headquarters, RWM&O Contractor, Building TES-1, TRW MS-24, 2650 Park Tower Drive, Suite 800, Vienna, VA 22180
53. Bruce Makenas, Duke Engineering Group, Box 350, MS-HO-40, Richland, Washington 99352
54. Roger McCormack, Duke Engineering and Services, Hanford, P.O. Box 350 (MSINR3-86), Richland, Washington 99352
55. Walter J. Mings, U.S. Department of Energy, Idaho Operations Office, 785 DOE Place, MS-1136, Room 56, Idaho Falls, ID 83401
56. Frank Moore, Westinghouse Savannah River Corp., 773A, Room B125, Aiken, SC 29808
57. Ron Moore, The RM Group, Inc., 12024 Broadwood Drive, Knoxville, TN 37922
58. James F. Morgan, Lawrence Livermore National Laboratory, 7000 East Avenue, L-175, Livermore, California 94550
59. Dick Murphy, Westinghouse Savannah River Corp., 707C, Room 237, Aiken, SC 29808
60. Ram Murphy, OCRUM, Office of Quality Assurance, RW-3, Department of Energy, Forrestal Building, Washington, DC 20585
61. D. A. Nitti, Department of Energy Headquarters, RWM&O Contractor, Building TES-1, TRW MS-24, 2650 Park Tower Drive, Suite 800, Vienna, VA 22180
62. David Norton, Houston Advanced Research Center, 4800 Research Forest Drive, The Woodlands, TX 77381
63. M. M. Pickrell, Los Alamos National Laboratory, P.O. Box 1663, NIS-5, MS-E540, Los Alamos, NM 87545
64. Bertram A. Pohl, Lawrence Livermore National Laboratory, 7000 East Avenue, L-059, Livermore, California 94550
65. Bob Rasmussen, Duke Engineering Group, Hanford Inc., P.O. Box 350, MS-R3-86, Richland, Washington 99351

66. P. M. Rinard, Los Alamos National Laboratory, P.O. Box 1663, NIS-5, MS-E540, Los Alamos, NM 87545
67. D. Rivas, Idaho National Engineering Lab, P.O. Box 1625, MS-1145, Idaho Falls, ID 83415
68. Thomas Sanders, Sandia National Laboratory, P.O. Box 5800, MS-0727, Albuquerque, NM 87185-0727
69. Kevin D. Seager, Sandia National Laboratory, P.O. Box 5800, MS-0716, Albuquerque, NM 87185-0716
70. M. M. Sevik, Carderock Division, Naval Surface Warfare Center, Code 70, Bethesda, MD 20084-5000
71. R. B. Stout, Lawrence Livermore National Laboratory, 7000 East Avenue, L-201, Livermore, California 94550
72. Ernesto Suarez, Pratt & Whitney, P.O. Box 109600, Mail Stop 716-87, West Palm Beach, FL 33410-9600
73. John H. Thompson, U.S. Department of Energy Headquarters, EM-37, Trevion Building, Room 345, 19901 Germantown Road, Germantown, MD 20874
74. S. A. Vance, Department of Energy Headquarters, RWM&O Contractor, Building TES-1, TRW MS-24, 2650 Park Tower Drive, Suite 800, Vienna, VA 22180
75. P. D. Wheatley, Idaho National Engineering Lab, P.O. Box 1625, MS-3135, Idaho Falls, ID 83415
76. Jeff Williams, Department of Energy-RW, 1000 Independence Avenue, SW, RW-46, Washington, DC 20585

77-78. Office of Scientific and Technical Information, U.S. Department of Energy, P.O. Box 62, Oak Ridge, TN 37831